

# Molecular reorganization of endocannabinoid signalling in Alzheimer's disease

Jan Mulder,<sup>1,\*</sup> Misha Zilberter,<sup>2,†</sup> Susana J. Pasquaré,<sup>3,4,†</sup> Alán Alpár,<sup>1,†</sup> Gunnar Schulte,<sup>5</sup> Samira G. Ferreira,<sup>6</sup> Attila Köfalvi,<sup>6</sup> Ana M. Martín-Moreno,<sup>3</sup> Erik Keimpema,<sup>1</sup> Heikki Tanila,<sup>7</sup> Masahiko Watanabe,<sup>8</sup> Ken Mackie,<sup>9</sup> Tibor Hortobágyi,<sup>10</sup> Maria L. de Ceballos<sup>3</sup> and Tibor Harkany<sup>1,2</sup>

<sup>1</sup> European Neuroscience Institute at Aberdeen, School of Medical Sciences, University of Aberdeen, Aberdeen AB25 2ZD, UK

<sup>2</sup> Division of Molecular Neurobiology, Department of Medical Biochemistry and Biophysics, Karolinska Institutet, S-17177 Stockholm, Sweden

<sup>3</sup> Department of Cellular, Molecular and Developmental Neuroscience and CIBERNED, Cajal Institute, CISC, Madrid, Spain

<sup>4</sup> Instituto de Investigaciones Bioquímicas de Bahía Blanca, Universidad Nacional del Sur and CONICET, Bahía Blanca, Argentina

<sup>5</sup> Department of Physiology and Pharmacology, Section for Receptor Biology and Signalling, Karolinska Institutet, S-17177 Stockholm, Sweden

<sup>6</sup> Centre for Neurosciences and Cell Biology of Coimbra, Faculty of Medicine, University of Coimbra, 3004-517 Coimbra, Portugal

<sup>7</sup> A. I. Virtanen Institute, University of Eastern Finland, F-70211 Kuopio, Finland

<sup>8</sup> Department of Anatomy, Hokkaido University School of Medicine, Sapporo 060-8638, Japan

<sup>9</sup> Gill Center for Neuroscience, Department of Psychological and Brain Sciences, Indiana University, Bloomington, IN 47405, USA

<sup>10</sup> Department of Clinical Neuroscience, Institute of Psychiatry, King's College London, London SE5 8AF, UK

\*Present address: Science for Life Laboratory, Karolinska Institutet, S-17177, Stockholm, Sweden.

†These authors contributed equally to this work.

Correspondence to: Dr Tibor Harkany,  
Department of Medical Biochemistry and Biophysics,  
Division of Molecular Neurobiology,  
Scheeles väg 1 A1,  
Karolinska Institutet,  
S-17177 Stockholm,  
Sweden  
E-mail: tibor.harkany@ki.se

Retrograde messengers adjust the precise timing of neurotransmitter release from the presynapse, thus modulating synaptic efficacy and neuronal activity. 2-Arachidonoyl glycerol, an endocannabinoid, is one such messenger produced in the postsynapse that inhibits neurotransmitter release upon activating presynaptic CB<sub>1</sub> cannabinoid receptors. Cognitive decline in Alzheimer's disease is due to synaptic failure in hippocampal neuronal networks. We hypothesized that errant retrograde 2-arachidonoyl glycerol signalling impairs synaptic neurotransmission in Alzheimer's disease. Comparative protein profiling and quantitative morphometry showed that overall CB<sub>1</sub> cannabinoid receptor protein levels in the hippocampi of patients with Alzheimer's disease remain unchanged relative to age-matched controls, and CB<sub>1</sub> cannabinoid receptor-positive presynapses engulf amyloid- $\beta$ -containing senile plaques. Hippocampal protein concentrations for the *sn*-1-diacylglycerol lipase  $\alpha$  and  $\beta$  isoforms, synthesizing 2-arachidonoyl glycerol, significantly increased in definite Alzheimer's (Braak stage VI), with ectopic *sn*-1-diacylglycerol lipase  $\beta$  expression found in microglia accumulating near senile plaques and apposing CB<sub>1</sub> cannabinoid receptor-positive presynapses. We found that microglia, expressing two 2-arachidonoyl glycerol-degrading enzymes, serine hydrolase  $\alpha/\beta$ -hydrolase domain-containing 6 and monoacylglycerol lipase, begin to surround senile plaques in probable Alzheimer's disease (Braak stage III). However, Alzheimer's pathology differentially impacts serine hydrolase  $\alpha/\beta$ -hydrolase

domain-containing 6 and monoacylglycerol lipase in hippocampal neurons: serine hydrolase  $\alpha/\beta$ -hydrolase domain-containing 6 expression ceases in neurofibrillary tangle-bearing pyramidal cells. In contrast, pyramidal cells containing hyperphosphorylated tau retain monoacylglycerol lipase expression, although at levels significantly lower than in neurons lacking neurofibrillary pathology. Here, monoacylglycerol lipase accumulates in CB<sub>1</sub> cannabinoid receptor-positive presynapses. Subcellular fractionation revealed impaired monoacylglycerol lipase recruitment to biological membranes in post-mortem Alzheimer's tissues, suggesting that disease progression slows the termination of 2-arachidonoyl glycerol signalling. We have experimentally confirmed that altered 2-arachidonoyl glycerol signalling could contribute to synapse silencing in Alzheimer's disease by demonstrating significantly prolonged depolarization-induced suppression of inhibition when superfusing mouse hippocampi with amyloid- $\beta$ . We propose that the temporal dynamics and cellular specificity of molecular rearrangements impairing 2-arachidonoyl glycerol availability and actions may differ from those of anandamide. Thus, enhanced endocannabinoid signalling, particularly around senile plaques, can exacerbate synaptic failure in Alzheimer's disease.

**Keywords:** glia; human; neurodegeneration; retrograde signalling; synapse

**Abbreviations:** ABHD6 = serine hydrolase  $\alpha/\beta$ -hydrolase domain-containing 6; DAGL = *sn*-1-diacylglycerol lipase; FAAH = fatty-acid amide hydrolase; IBA-1 = ionized Ca<sup>2+</sup>-binding adaptor molecule-1; MAP2 = microtubule-associated protein 2; NAPE-PLD = N-acyl phosphatidylethanolamide-specific phospholipase D; PSD95 = postsynaptic density protein of 95 kDa; SNAP25 = synaptosomal-associated protein of 25 kDa; TRPV1 = transient receptor potential cation channel subfamily V member 1

## Introduction

Alzheimer's disease is the most common form of age-related dementia. Although two competing hypotheses exist as to the molecular sequel behind neuronal demise in Alzheimer's disease (Small and Duff, 2008), the ultimate and invariable outcome of both intracellular tau hyperphosphorylation, and overt production and extracellular release of amyloid- $\beta$  is impaired synaptic communication, particularly in the hippocampus (Oddo *et al.*, 2003; Walsh and Selkoe, 2004). Oligomeric amyloid- $\beta$  can target excitatory synapses (Shemer *et al.*, 2006), where amyloid- $\beta$  disrupts the molecular machinery underpinning both presynaptic neurotransmitter release and postsynaptic responsiveness, thus impairing various forms of short- and long-term synaptic plasticity (Walsh *et al.*, 2002; Shemer *et al.*, 2006). A causal relationship between amyloid- $\beta$ -induced NMDA and AMPA receptor removal and dephosphorylation (Kamenetz *et al.*, 2003; Snyder *et al.*, 2005; Hsieh *et al.*, 2006; Gu *et al.*, 2009) and impaired intracellular Ca<sup>2+</sup> signalling in the postsynapse (Kuchibhotla *et al.*, 2008), predominantly in dendritic spines receiving excitatory inputs, has been identified as a determinant of amyloid- $\beta$ -induced synaptic dysfunction.

The temporal dynamics of neurotransmitter release at both excitatory and inhibitory synapses are controlled by retrograde signalling networks (Alger, 2002), with retrograde messengers liberated from the subsynaptic dendrite in temporal cohesion with postsynaptic spike timing (Kano *et al.*, 2009). Endocannabinoid signalling is one such mechanism widely distributed in rodent (Katona *et al.*, 2006), primate (Harkany *et al.*, 2005) and human brains (Ludanyi *et al.*, 2011). Transgenic analyses (Gao *et al.*, 2010; Tanimura *et al.*, 2010) reveal that 2-arachidonoyl glycerol is a particularly efficacious endocannabinoid to tune synaptic communication in the hippocampus. The canonical pathway of 2-arachidonoyl glycerol metabolism posits 2-arachidonoyl glycerol synthesis by Ca<sup>2+</sup>-dependent

*sn*-1-diacylglycerol lipases  $\alpha$  and  $\beta$  (DAGLs) (Bisogno *et al.*, 2003), with DAGLs anchored at the neck of dendritic spines (Uchigashima *et al.*, 2007). Once released, 2-arachidonoyl glycerol engages CB<sub>1</sub> cannabinoid receptors at glutamatergic as well as GABAergic presynapses (Kano *et al.*, 2009). Monoacylglycerol lipase (Dinh *et al.*, 2002) and the serine hydrolase  $\alpha/\beta$ -hydrolase domain-containing 6 (ABHD6) are recruited to pre- (Hashimoto *et al.*, 2007) and postsynaptic sites (Marrs *et al.*, 2010), respectively, to terminate 2-arachidonoyl glycerol signalling.

Age-related learning and memory deficits upon CB<sub>1</sub> cannabinoid receptor deletion (Bilkei-Gorzo *et al.*, 2005) or phytocannabinoid administration (Wise *et al.*, 2009) illustrate the physiological significance of endocannabinoid signalling in the ageing brain. In Alzheimer's disease, endocannabinoids may exert dual roles (Bisogno and Di Marzo, 2008). Increased endocannabinoid availability appears beneficial in reducing pro-inflammatory microglia transformation and activity through a CB<sub>2</sub> cannabinoid receptor-dependent mechanism (Ramirez *et al.*, 2005; Halleskog *et al.*, 2011). Alternatively, CB<sub>1</sub> cannabinoid receptor modulation can gate amyloid- $\beta$  neurotoxicity and protect against amyloid- $\beta$ -induced amnesia in hippocampal learning tasks (Mazzola *et al.*, 2003; Micale *et al.*, 2010). While CB<sub>1</sub> cannabinoid receptor activation during ongoing neurodegeneration clearly improves cognitive outcome by inhibiting neuronal apoptosis and gliosis, CB<sub>1</sub> cannabinoid receptor agonist administration during advanced neurodegeneration could instead worsen amyloid- $\beta$ -induced neuronal demise by inhibiting residual neuronal activity (van der Stelt *et al.*, 2006). Nevertheless, experimental evidence unequivocally identifying the impact of amyloid- $\beta$  on endocannabinoid-mediated forms of hippocampal synaptic plasticity is lacking.

Modifications to CB<sub>1</sub> cannabinoid receptor expression and signalling efficacy in Alzheimer's disease are ambiguous (Westlake *et al.*, 1994; Lee *et al.*, 2010). In addition, coordinated expression and subcellular distribution of CB<sub>1</sub> cannabinoid receptors, DAGLs, ABHD6 and monoacylglycerol lipase, and their relationship to

retrograde signalling in Alzheimer's disease, remain essentially unexplored. We hypothesized a functional relationship between errant 2-arachidonoyl glycerol signalling and synaptic impairment in Alzheimer's disease: amyloid- $\beta$  could impact  $\text{Ca}^{2+}$ -dependent 2-arachidonoyl glycerol synthesis and release, while cytoskeletal damage might alter subcellular DAGL, monoacylglycerol lipase and/or ABHD6 recruitment, thus disrupting the dynamics of 2-arachidonoyl glycerol signalling. Irrespective of the primary pathogenic cascade, molecular reorganization of 2-arachidonoyl glycerol signalling networks might be detrimental to maintain synaptic responsiveness and plasticity. We have tested these hypotheses by dissecting the molecular machinery of 2-arachidonoyl glycerol signalling in post-mortem human brains with Alzheimer's pathology, in transgenic mouse models and upon acute amyloid- $\beta$  challenge to hippocampal neurons.

## Materials and methods

### Human tissues

Hippocampal tissue samples were obtained from patients with Alzheimer's disease and age-matched controls (without clinical signs of neuropsychiatric disease) at the London Neurodegenerative Diseases Brain Bank (Supplementary Table 1). Neuropathological and histochemical examination, including classification of amyloid- $\beta$  plaque burden (Supplementary Fig. 1A), tau pathology (Supplementary Table 1) and synaptic impairment (Supplementary Fig. 1B–E), was performed as described (Supplementary Material). Tissue blocks or entire hippocampi were immersion fixed in 4% paraformaldehyde in 0.1M phosphate buffer (pH 7.4) for 48–72 h at 4°C, followed by long-term storage in 0.1 M phosphate buffer to which 0.1%  $\text{NaN}_3$  had been added. Alternatively, native tissue blocks (2–3  $\text{cm}^3$ ) of ~1 cm thickness from the other hemisphere were stored at –80°C until processing for biochemical analysis.

### APdE9 mice

Male APPswe/PS1dE9 (APdE9) transgenic mice and littermate controls aged 7 or 14 months were used ( $n = 26$  animals in total; ethical documentation of *in vivo* studies can be found in online Supplementary Material). APdE9 mice were generated by heterozygously co-expressing mutant amyloid-precursor protein (KM593/594NL) and an exon 9 deletion variant of presenilin 1, both associated with familial Alzheimer's disease (Jankowsky *et al.*, 2004).

### Immunohistochemistry and imaging

Multiple immunofluorescence histochemistry on human temporal lobe sections containing the hippocampal formation was performed by applying select combinations of primary antibodies (Supplementary Fig. 2, Supplementary Table 2) according to standard protocols (Harkany *et al.*, 2003, 2005; Keimpema *et al.*, 2010; Halleskog *et al.*, 2011). Single x–y plane or orthogonal z image stacks were captured, after quenching tissue autofluorescence (Supplementary Fig. 3), by laser-scanning microscopy (710LSM, Zeiss) as described in the online Supplementary Material. Three dimensional reconstruction and rendering of dendrite segments to specify the spatial relationships of DAGL $\alpha$ /DAGL $\beta$  or monoacylglycerol lipase immunoreactivities was

performed using the BioVis3D reconstruction package (Montevideo) according to the specific imaging criteria (Supplementary Methods).

### Acute brain slice preparation and electrophysiology

Patch clamp recordings, differential interference contrast imaging and stimulus protocols in hippocampal slices from postnatal 14- or 16-day-old mouse brains were performed as described (Supplementary Methods).

### Western blotting

Protein samples prepared from human or mouse hippocampi were analysed under denaturing conditions. Western blot analysis was undertaken as described (Supplementary Methods) with primary antibodies listed in Supplementary Table 2. Blots were scanned on a Licor Odyssey-IR imager and quantified with ImageJ1.32j.

### WNT-3A stimulation and gene expression profiling in microglia

Primary microglia were isolated from newborn mouse brains (Halleskog *et al.*, 2011). Cultures typically contained >95% microglia, as validated by cytochemistry with *Griffonia simplicifolia* isolectin B4 (Sigma). Three independent harvests of primary microglia were seeded in six-well plates and challenged 24 h after plating. Serum-deprived microglia were treated with either 0.1% bovine serum albumin (vehicle control) or 300 ng/ml recombinant WNT-3A for 6 h. RNA was prepared and analysed on an Affimetrix Mouse Gene 1.0 ST Array (Halleskog *et al.*, 2011). Real-time quantitative polymerase chain reaction analysis was performed as reported previously with custom-designed primers (Keimpema *et al.*, 2010). N13 microglia-like cells (Halleskog *et al.*, 2011) were exposed to fibrillar amyloid- $\beta_{1-42}$  at 100 nM final concentration for 48 h.

### 2-Arachidonoyl glycerol degradation in Alzheimer's brains

Biochemical studies were conducted in an independent cohort of human cortical samples (Supplementary Material). Neurohistopathological evaluation and disease classification were as above. Frontal cortices were mechanically homogenized (10%) in Tris–HCl (20 mM, pH 7.2) containing 0.32 M sucrose and protease inhibitors, and centrifuged to eliminate nuclei and cellular debris (1000g, 10 min, 4°C). Supernatants were ultracentrifuged (100 000g, 60 min, 4°C) to obtain membrane and soluble fractions, both presenting 2-arachidonoyl glycerol-degrading activity (Blankman *et al.*, 2007). Protein concentrations were determined by Bradford's colorimetric method (Bradford, 1976). The 2-arachidonoyl glycerol-degrading activity was assessed by incubating sample fractions (10  $\mu\text{g}$  protein) in a solution containing Tris–HCl (10 mM, pH 7.2), 1 mM ethylenediaminetetraacetic acid, fatty acid-free bovine serum albumin (1.25 mg/ml), [ $^3\text{H}$ ]2-arachidonoyl glycerol ([1,2,3- $^3\text{H}$ ]glycerol, 25  $\mu\text{M}$ , 40 Ci/mmol specific activity; New England Nuclear) in a final volume of 200  $\mu\text{l}$  for 15 min at 37°C. Identical conditions were used to assess anandamide degrading activity using [ $^3\text{H}$ ]anandamide ([1- $^3\text{H}$ ]ethanolamine, 25  $\mu\text{M}$ , 40 Ci/mmol specific activity; ARC Inc.). Reactions were stopped by 400  $\mu\text{l}$  chloroform:methanol (2:1, v/v) and vigorous vortexing. Fractions either containing [1,2,3- $^3\text{H}$ ]glycerol/[1- $^3\text{H}$ ]ethanolamine (top) or non-hydrolyzed [ $^3\text{H}$ ]2-arachidonoyl glycerol/[ $^3\text{H}$ ]anandamide (bottom/organic) were separated by

centrifugation (2000 g, 10 min, 4°C), transferred into scintillation vials and radioactivity measured by liquid scintillation spectroscopy. Actual experimental conditions were selected from pilot experiments assaying the relationship of substrate and protein concentrations to identify optimal 2-arachidonoyl glycerol-degrading enzymatic activity (data not shown), and favoured assay conditions allowing ~50% of 2-arachidonoyl glycerol converted into glycerol in membrane fractions from control brains. JZL184 (5 µM) (Long *et al.*, 2009) or URB602 (1 mM) (King *et al.*, 2007) served to determine the specific contribution of monoacylglycerol lipase to 2-arachidonoyl glycerol degradation. URB597 (20 nM) (Mor *et al.*, 2004) was used to test the changes in anandamide-degrading activity in Alzheimer's disease brains. Enzyme activity was expressed as picomole [1,2,3-<sup>3</sup>H]glycerol formed/mg protein/15 min and picomole [<sup>3</sup>H]ethanolamine formed/mg protein/15 min, respectively. Human amyloid-β<sub>1–40</sub> (PolyPeptides) were diluted and used as described for amyloid-β<sub>1–42</sub> (Supplementary Methods). Methods to assess transient receptor potential cation channel subfamily V member 1 (TRPV<sub>1</sub>) channel binding in post-mortem hippocampal samples are provided in the online Supplementary Material.

## Statistical analysis

Data were analysed using Statistical Package for the Social Sciences 17.0 (SPSS Inc.). Integrated optical density of immunoreactive targets in Western blot experiments, and decay constants from electrophysiology measurements were evaluated using Student's *t*-test (on independent samples). Linear regression analysis of CB<sub>1</sub> cannabinoid receptor, DAGLs and monoacylglycerol lipase isoforms, synaptic markers, disease stages and/or post-mortem delay (Supplementary Fig. 4) was performed by defining Pearson's correlation coefficient. Data were expressed as mean ± SEM. *P* < 0.05 was considered statistically significant.

## Results

Here, we focus on molecular rearrangements of 2-arachidonoyl glycerol signalling networks progressively affecting synaptic neurotransmission during Alzheimer's disease in human brain and experimental models of amyloid-β synaptotoxicity. We also present data on N-acyl phosphatidylethanolamide-specific phospholipase D (NAPE-PLD), fatty-acid amide hydrolase (FAAH) and TRPV<sub>1</sub>, significantly extending available knowledge on Alzheimer's-related modifications to anandamide signalling (Benito *et al.*, 2003; Ramirez *et al.*, 2005) in Supplementary Fig. 5. Changes of CB<sub>2</sub> cannabinoid receptor expression in this cohort of subjects with Alzheimer's disease have recently been reported elsewhere (Halleskog *et al.*, 2011).

### CB<sub>1</sub> cannabinoid receptor expression is unchanged in Alzheimer's disease

Cellular mapping studies, combined with ultrastructural analysis, unequivocally position CB<sub>1</sub> cannabinoid receptors presynaptically in both excitatory and inhibitory nerve endings of rodent (Katona *et al.*, 2006), primate (Harkany *et al.*, 2005) and human hippocampus (Ludanyi *et al.*, 2011). However, the impact of ageing or Alzheimer pathology on CB<sub>1</sub> cannabinoid receptor expression and (sub-)cellular distribution in the human hippocampus remain ambiguous (Westlake *et al.*, 1994; Lee *et al.*, 2010).

We have studied clinicopathologically-verified patient material consisting of 10 subjects classified as controls (≤ Braak I stage) aged 52–96 years, nine subjects presenting Braak stage III/IV pathology and aged 72–105 years, as well as nine patients with pathological indices of Braak stage VI and aged 69–90 years (Supplementary Table 1). Braak stage III/IV and Braak stage VI patients had significantly increased amyloid-β levels (Supplementary Fig. 1A) and synaptic modifications as suggested by decreased levels of synaptosomal-associated protein of 25 kDa (SNAP25) (Garbelli *et al.*, 2008) and postsynaptic density protein of 95 kDa (PSD95) (Sampedro *et al.*, 1982), pre- and postsynaptic markers, respectively (Supplementary Fig. 1C and D).

Western analysis demonstrated CB<sub>1</sub> cannabinoid receptor expression in the aged human hippocampus (Fig. 1A). CB<sub>1</sub> cannabinoid receptors were of 52 kDa molecular weight suggesting that mature, non-truncated receptors were detected in post-mortem brain homogenates (Fig. 1A and B). CB<sub>1</sub> cannabinoid receptor levels remained unchanged in patients with Braak stage III/IV or Braak stage VI pathology (Fig. 1B). We performed correlation analysis between SNAP25, PSD95 and CB<sub>1</sub> cannabinoid receptors to test whether individual variations in CB<sub>1</sub> cannabinoid receptor levels may be related to those of SNAP25 or PSD95 at excitatory synapses. However, CB<sub>1</sub> cannabinoid receptor expression did not correlate with that of either SNAP25 (Supplementary Fig. 1E) or PSD95 (data not shown).

Immunohistochemistry revealed a dense meshwork of CB<sub>1</sub> cannabinoid receptor<sup>+</sup> axons with CB<sub>1</sub> cannabinoid receptors particularly enriched in presynapses that contained synaptophysin, a pan-presynaptic marker (Schubert *et al.*, 1991), in the strata pyramidale and radiatum of the Ammon's horn 1–3 subfields (Fig. 2A and B; Supplementary Fig. 6A–A<sub>3</sub>), and the stratum moleculare of the fascia dentata (Supplementary Fig. 7A) of aged human subjects. High-resolution laser-scanning microscopy confirmed that CB<sub>1</sub> cannabinoid receptors localized to synaptophysin<sup>+</sup> presynapses targeting either the perisomatic segment (Fig. 2C–C<sub>3</sub>) or distal dendrites (Fig. 2D–D<sub>3</sub>) of pyramidal neurons. Accordingly, CB<sub>1</sub> cannabinoid receptor<sup>+</sup>/microtubule-associated protein 2<sup>+</sup> (MAP2<sup>+</sup>) double-labelled structures were not observed (MAP2 is a ubiquitous somatodendritic marker of neurons) (Peng *et al.*, 1986). CB<sub>1</sub> cannabinoid receptor distribution in Braak stage III/IV/Braak stage VI cases was unaltered; CB<sub>1</sub> cannabinoid receptor<sup>+</sup> axons coursed in both soma-rich laminae, including the stratum granulosum (Fig. 2E) and receptive fields (e.g. stratum moleculare; Fig. 2E). Notably, CB<sub>1</sub> cannabinoid receptor<sup>+</sup> axons appeared to engulf senile plaques (Fig. 2E<sub>1</sub>–E<sub>3</sub>) with CB<sub>1</sub> cannabinoid receptor<sup>+</sup> bouton-like varicosities commonly situated within the amyloid-β-dense plaque cores. Therefore, we conclude that CB<sub>1</sub> cannabinoid receptor expression and axonal distribution remain largely unaffected in Alzheimer's disease.

### DAGLβ but not DAGLα redistribution in Alzheimer's disease

The long-held view of 2-arachidonoyl glycerol biosynthesis posits DAGLs as Ca<sup>2+</sup>-regulated enzymes synthesizing this endocannabinoid (Bisogno *et al.*, 2003). DAGLs reside in the perisynaptic



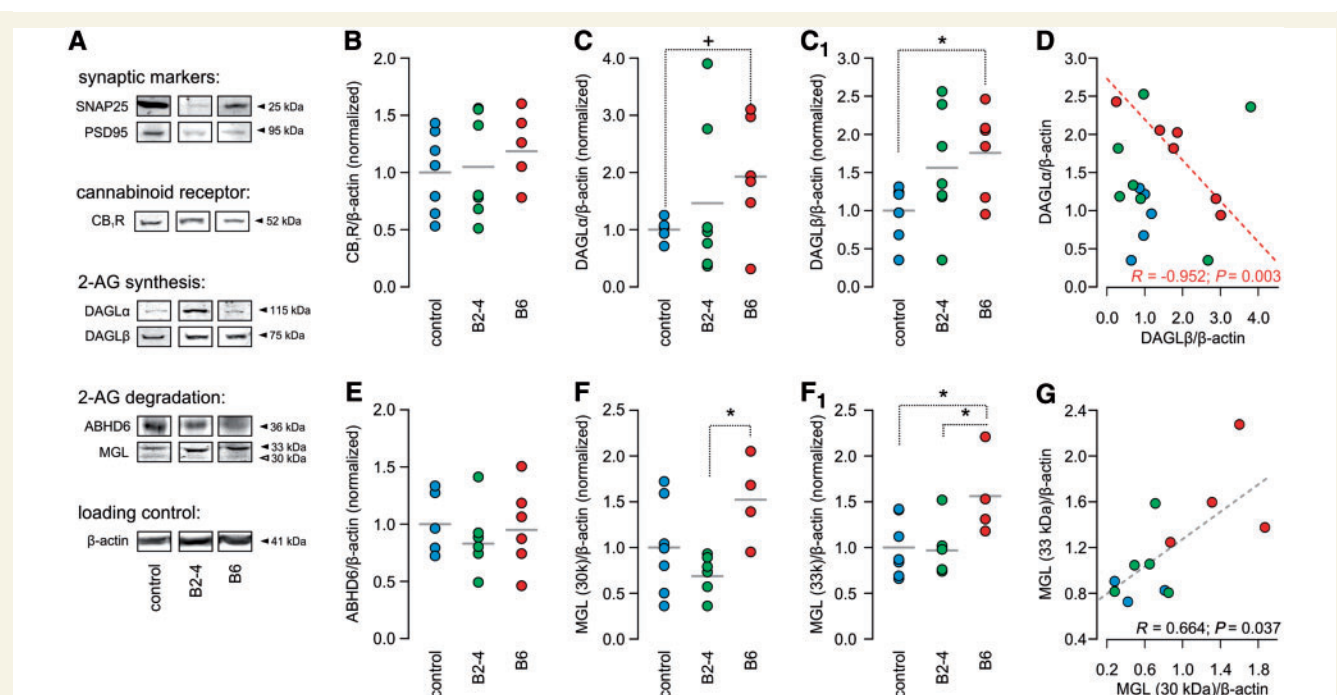


**Figure 1** Changes in DAGL and monoacylglycerol lipase protein expression in human hippocampus coincide with Alzheimer's progression. (A) Representative images of molecular targets resolved by western blotting. Data (in kiloDaltons) indicate the calculated molecular weights of the molecules of interest. Solid and open arrowheads identify monoacylglycerol lipase's 33 kDa and 30 kDa isoforms, respectively. Calculated molecular weights corresponded with those measured in particular experiments in all cases. We did not observe modifications to the molecular weights of any of the targets analysed (otherwise represented as vertical size shifts) when comparing data from control, and cohorts with moderate or severe Alzheimer's disease [Braak stage III/IV (B2–4) and Braak stage VI (B6), respectively]. Normalized expression (average of controls = 1.0) of CB<sub>1</sub> cannabinoid receptors (CB<sub>1</sub>R) (B), DAGL $\alpha$  (C;  $^{+}P < 0.1$ ), DAGL $\beta$  (C<sub>1</sub>), ABHD6 (E), 30 kDa (F) and 33 kDa (F<sub>1</sub>) isoforms of monoacylglycerol lipase. Individual data points and their colour coding correspond to post-mortem cases listed in Supplementary Table 1.  $\beta$ -actin was used as loading control to normalize our data (Supplementary Fig. 1B and B<sub>1</sub>). Horizontal lines represent the mean value of particular patient cohorts. (D) DAGL $\alpha$  and DAGL $\beta$  levels correlated positively in controls (not marked), lost correlation in Braak stage III/IV, while exhibited a strong negative expressional relationship in Braak stage VI (red dashed line). (G) Monoacylglycerol lipase isoform expression positively correlates during Alzheimer's progression.  $^{*}P < 0.05$  (Student's  $t$ -test). 2-AG = 2-arachidonoyl glycerol.

annulus, a proximal zone surrounding the postsynaptic density at CB<sub>1</sub> cannabinoid receptor<sup>+</sup> excitatory synapses (Uchigashima *et al.*, 2007), also in human brain (Ludanyi *et al.*, 2011). Epilepsy-induced sclerotic neurodegeneration in human brain reduces DAGL $\alpha$  but not DAGL $\beta$  expression by ~60% suggesting that impaired 2-arachidonoyl glycerol synthesis may occur under disease conditions (Ludanyi *et al.*, 2008).

We have tested this possibility by analysing DAGL $\alpha$  and DAGL $\beta$  protein expression in Braak stage III/IV, Braak stage VI and age-matched control brains (Fig. 1A, C and C<sub>1</sub>). We found a gradual increase in the protein levels of both enzymes, paralleling Alzheimer's progression [DAGL $\alpha$ :  $145.4 \pm 50.9\%$  of control,  $n = 7$  (Braak stage III/IV),  $193.9 \pm 41.9\%$  of control,  $n = 6$ ,  $P = 0.076$  versus control (Braak stage VI); DAGL $\beta$ :  $155.1 \pm 29.1\%$  of control,  $n = 7$  (Braak stage III/IV);  $175.9 \pm 23.7\%$  of control,  $n = 6$ ,  $P = 0.015$  versus control (Braak stage VI); Fig. 1C and C<sub>1</sub>]. Next, we explored whether DAGL $\alpha$  expression correlates with that of DAGL $\beta$ . Analysis of discrete subject cohorts revealed the lack of an expressional relationship between the two enzymes in control or Braak stage III/IV brains (Fig. 1D). In contrast, we found a

strong inverse relationship between DAGL $\alpha$  and DAGL $\beta$  protein levels in Braak stage VI brains (Fig. 1D). These findings suggest that either DAGL $\alpha$  is replaced by DAGL $\beta$  postsynaptically or DAGL $\alpha$  and DAGL $\beta$  segregate to distinct cell types with independent expressional control for DAGLs in Alzheimer's disease.

Multiple immunofluorescence histochemistry using affinity-pure antibodies (Supplementary Fig. 2), and appropriate histochemical (Supplementary Fig. 3) and imaging (Supplementary Fig. 6B) controls, in the Ammon's horn 1–3 subfields of the aged human hippocampus and fascia dentata (Fig. 3A and Supplementary Fig. 7B–B<sub>2</sub>) revealed DAGL $\alpha$ <sup>+</sup> and DAGL $\beta$ <sup>+</sup> puncta along the dendritic trees of pyramidal neurons (Fig. 3B–B<sub>2</sub>) and granule cells (Supplementary Fig. 7B–B<sub>2</sub>). The density of DAGL $\alpha$ <sup>+</sup> puncta exceeded that of DAGL $\beta$ <sup>+</sup> structures (Fig. 3B–B<sub>2</sub>, C<sub>1</sub>–C<sub>3</sub> and E<sub>1</sub>). High-resolution microscopy along individual MAP2<sup>+</sup> dendrite segments showed frequent DAGL $\alpha$ /DAGL $\beta$  co-localization (Fig. 3C–C<sub>3</sub>). Three dimensional reconstruction of select dendrites upon capturing consecutive images in orthogonal stacks verified that both DAGL $\alpha$  and DAGL $\beta$  were localized within dendritic compartments and accumulated at the stem of dendritic spines (Fig. 3D and D<sub>1</sub>).

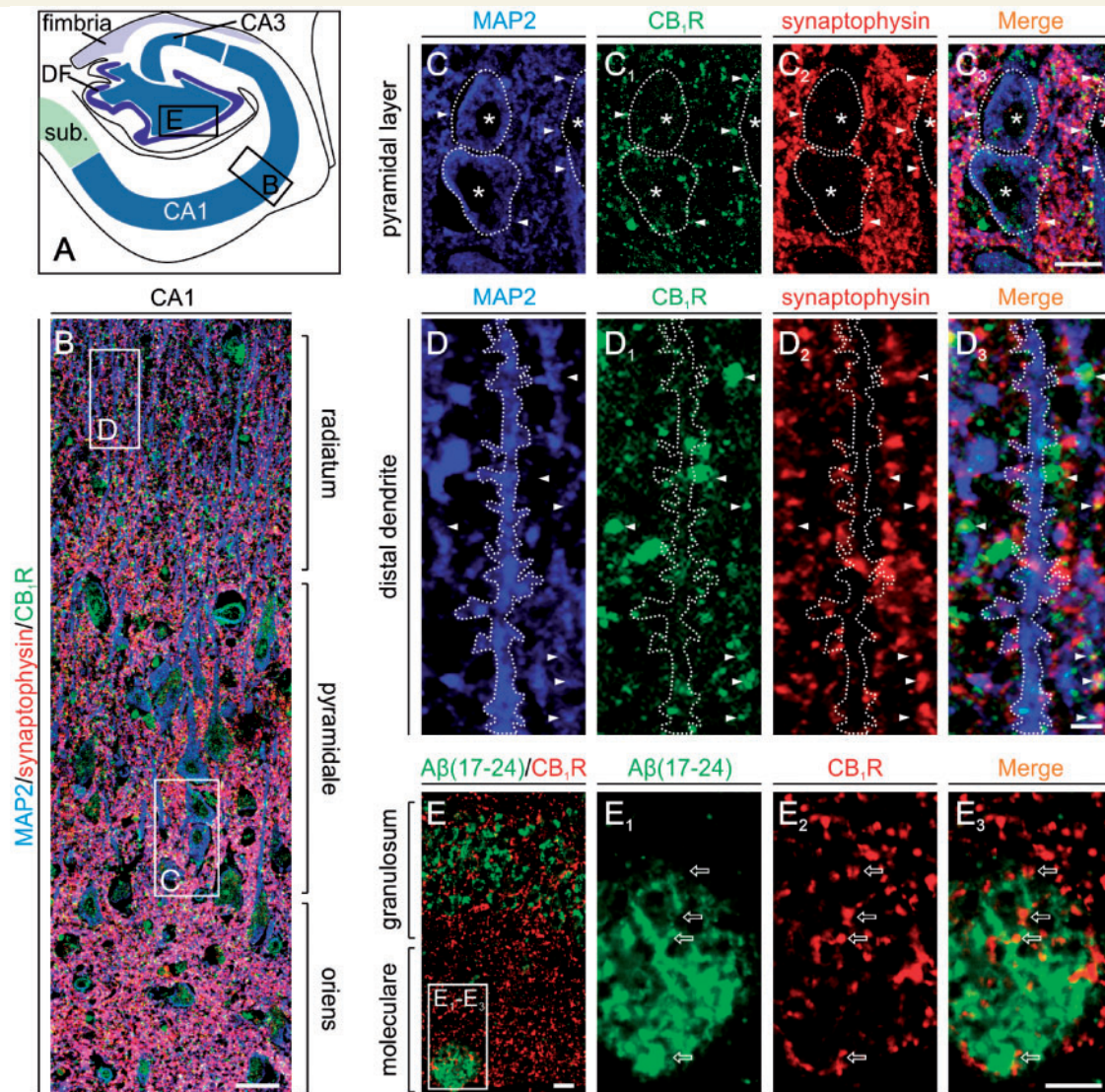


**Figure 2** CB<sub>1</sub> cannabinoid receptor distribution in aged human hippocampus and in Alzheimer's disease. (A) Schema of the human hippocampal formation. Open rectangles identify the general location of images in B and E. (B) CB<sub>1</sub> cannabinoid receptor (CB<sub>1</sub>R) immunoreactivity overlaps with synaptophysin<sup>+</sup> nerve terminals targeting the perisomatic region (C) as well as apical dendrites (D) of Ammon's horn 1 pyramidal neurons. High-resolution microscopy reveals CB<sub>1</sub> cannabinoid receptor<sup>+</sup>/synaptophysin<sup>+</sup> terminals (arrowheads) around pyramidal cell perikarya (C–C<sub>3</sub>) and dendrites (D–D<sub>3</sub>). Note the mutually exclusive localization of CB<sub>1</sub> cannabinoid receptors and MAP2<sup>+</sup> dendrites. Dashed lines encircle neuronal somata (C) and dendrite (D). Asterisks in C are overlain on neuronal nuclei. (E) CB<sub>1</sub> cannabinoid receptor<sup>+</sup> afferents engulf cells in the granular layer abundantly immunoreactive for amyloid-β<sub>17–24</sub> [Aβ(17–24)], likely localizing intracellular amyloid precursor protein, as well as amyloid-β<sub>17–24</sub><sup>+</sup> senile plaque (open rectangle). (E<sub>1</sub>–E<sub>3</sub>) The density of CB<sub>1</sub> cannabinoid receptor<sup>+</sup> axons and synapses appear unchanged in the proximity of senile plaques. Instead, CB<sub>1</sub> cannabinoid receptor<sup>+</sup> processes appear to accumulate locally around, and even penetrate senile plaques (arrows). CA = Ammon's horn; DF = dentate fascia; sub = subiculum. Scale bars = 20 μm (B, E and E<sub>3</sub>), 12 μm (C<sub>3</sub>), 4 μm (D<sub>3</sub>).

Quantitative morphometry showed that the Pearson's correlation coefficient of dual-labelled structures only marginally differs from 0, suggesting limited (if any) correlation (co-regulation) between signal intensities for DAGLα and DAGLβ (Fig. 3E). We quantitatively verified a higher density of DAGLα than DAGLβ along apical dendrite profiles of pyramidal cells in the Ammon's horn 1 subfield stratum radiatum (Fig. 3E<sub>1</sub> and see Fig. 3B–B<sub>2</sub>). Here,  $24.0 \pm 3.9\%$  of DAGLα<sup>+</sup> postsynaptic (MAP2<sup>+</sup>) puncta contained

DAGLβ (Fig. 3E<sub>2</sub>). In contrast,  $47.7 \pm 3.1\%$  of DAGLβ<sup>+</sup> structures were dual labelled, suggesting that DAGLα can drive DAGLβ recruitment to sites of co-localization.

The distribution of DAGLα immunoreactivity remained largely unchanged in Alzheimer's disease, including around senile plaques where DAGLα immunoreactivity has been found scattered in amyloid-β-laden territories (Fig. 3F). In contrast, DAGLβ immunoreactivity accumulated in small-diameter cell-like structures



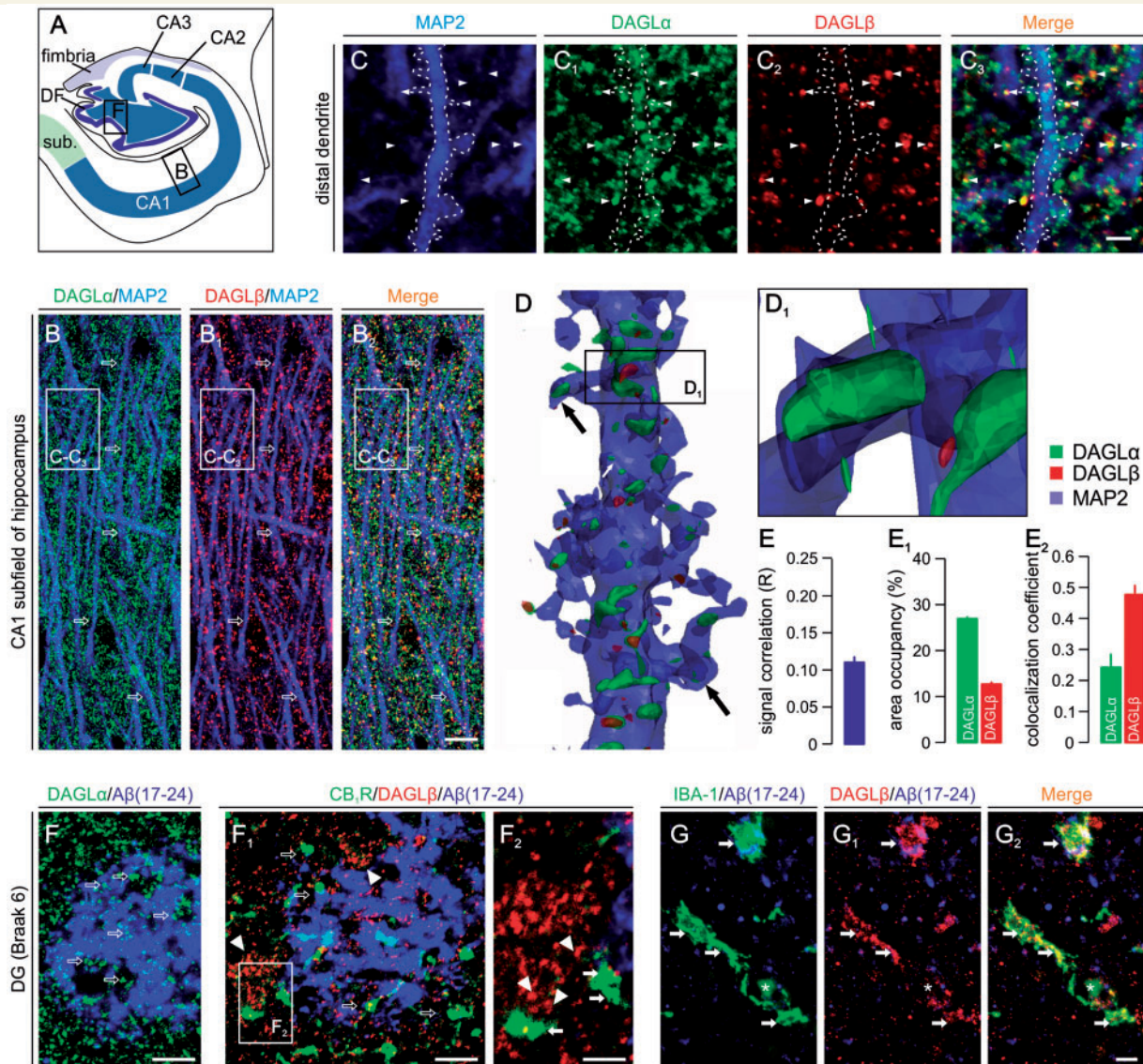


**Figure 3** Differential DAGL $\alpha$  and DAGL $\beta$  expression and localization in aged human hippocampus and in Alzheimer's disease. (A) Schematic overview of hippocampal subfields with open rectangles identifying the localization of dendritic fields shown in B and F. (B) MAP2 $^{+}$  dendritic shafts (arrows) are embedded in a fine meshwork of DAGL $\alpha^{+}$  and/or DAGL $\beta^{+}$  puncta, with the density of DAGL $\alpha$  immunoreactivity surpassing that of DAGL $\beta$  in the aged human hippocampus (control). (C) High-resolution imaging reveals coexistence of DAGL $\alpha$  and DAGL $\beta$  (arrowheads) in MAP2 $^{+}$  compartments. (D) 3D reconstruction of a MAP2 $^{+}$  pyramidal dendrite verifies the post-synaptic recruitment of DAGLs, and high-power rendering positions both DAGL $\alpha$  and DAGL $\beta$  in the dendritic spine neck (D $_1$ ). (E) Pearson's correlation coefficient suggests moderate positive correlation between the fluorescence maxima of DAGL $\alpha$  and DAGL $\beta$ . (E $_1$  and E $_2$ ) Area occupancy and co-localization coefficients for DAGL $\alpha$  and DAGL $\beta$  immunoreactivities verify the greater abundance of DAGL $\alpha$ , and reveal differences in their probability of co-localization, respectively. Data were expressed as means  $\pm$  SEM. (F) The distribution of DAGL $\alpha$  (arrowheads) does not change around amyloid- $\beta_{17-24}^{+}$  senile plaques. However, DAGL $\beta$  immunoreactivity focally concentrates in periplaque regions (F $_1$ ) in small-diameter cell-like structures (arrowheads, F $_1$ ) but not CB $_1$  cannabinoid receptor $^{+}$  (CB $_1$ R) processes (open arrows). Such DAGL $\beta^{+}$  cells closely appose (arrowheads, F $_2$ ) CB $_1$  cannabinoid receptor $^{+}$  axon terminals (arrows, F $_2$ ), and, based on their IBA-1 expression, were identified as activated microglia in Alzheimer's brains (arrows, G–G $_2$ ). Asterisks in G–G $_2$  pinpoint the soma of the microglial cell. CA = Ammon's horn; DF = dentate fascia; sub = subiculum. Scale bars = 40  $\mu$ m (B $_2$ ), 10  $\mu$ m (F and F $_1$ ), 4  $\mu$ m (C $_3$ , F $_2$  and G $_3$ ).

associated with senile plaques and apposing CB $_1$  cannabinoid receptor $^{+}$  axons (Fig. 3F $_1$  and F $_2$ ). By using ionized Ca $^{2+}$ -binding adaptor molecule-1 (IBA-1) we demonstrate that activated microglia (Xu *et al.*, 2008) frequently surrounding senile plaques express

DAGL $\beta$  in Braak stage VI brains (Fig. 3G–G $_2$ ). Together, these findings suggest that both DAGLs can coexist in dendritic spines of hippocampal neurons in the aged human hippocampus. In addition, microglia represent a novel cellular component

participating in 2-arachidonoyl glycerol biosynthesis in Alzheimer's disease. The specific accumulation of DAGL $\beta$ <sup>+</sup> microglia around senile plaques could lead to the focal enhancement of 2-arachidonoyl glycerol signalling, affecting neuronal excitability (Busche *et al.*, 2008), unless compensated by molecular rearrangements in 2-arachidonoyl glycerol-degrading enzymatic capacity in Alzheimer's brains.

## ABHD6 expression in Alzheimer's disease

ABHD6 is a recently characterized serine hydrolase degrading 2-arachidonoyl glycerol in the nervous system (Marrs *et al.*, 2010). While activity-based protein profiling identified ABHD6 as a candidate to hydrolyse 2-arachidonoyl glycerol in microglia-like cells, follow-up histochemical studies in rodent brain identified the somatodendritic domain of neurons as major, postsynaptic foci accumulating ABHD6 (Marrs *et al.*, 2010). Western blotting demonstrated that ABHD6 protein is present in the aged human hippocampus (Fig. 1A and E). Comparative analysis revealed unchanged ABHD6 levels across Braak stage III/IV, Braak stage VI and age-matched control tissues (Fig. 1A and E). However, these findings do not exclude the possibility that neuronal and glial ABHD6 expression differentially contribute to total ABHD6 levels in control versus Alzheimer's brains.

We show, by using affinity-pure anti-ABHD6 antibodies (Marrs *et al.*, 2010), ABHD6-like immunoreactivity decorating the somatic membrane and apical dendrites of pyramidal cells in the hippocampus of aged humans (Fig. 4A–A<sub>2</sub>). We found Alzheimer's progression associated with a gradual decrease of ABHD6-like immunoreactivity in hippocampal neurons (Fig. 4B and B<sub>1</sub>). Notably, the distribution of ABHD6 and AT8, the latter identifying tau hyperphosphorylated at Ser202/Thr205 residues in degenerating neurons (Goedert *et al.*, 1989), is mutually exclusive in Braak stage VI brain, suggesting that Alzheimer-related cytoskeletal damage can arrest ABHD6 expression (Fig. 4C and C<sub>1</sub>). In contrast, ABHD6<sup>+</sup> small diameter, multipolar cells lacking MAP2 accumulate in Alzheimer's brains (Fig. 4B and B<sub>1</sub>). We demonstrated that microglia can express ABHD6 (particularly in Braak stage VI) by revealing an intricate network of ABHD6<sup>+</sup>/IBA-1<sup>+</sup> but MAP2<sup>−</sup> microglia end-feet scattered around hippocampal neurons (Fig. 4B<sub>1</sub> and B<sub>2</sub>). In addition, we found that amyloid- $\beta$ -containing neuritic plaques attract ABHD6<sup>+</sup>/IBA-1<sup>+</sup> microglia, which accumulate both around and within senile plaques (Fig. 4D–D<sub>3</sub>). In summary, our data uncover a postsynaptic expression site for ABHD6 in neurons of the aged human hippocampus, as well as widespread ABHD6 expression by activated microglia in Alzheimer's disease.

## Monoacylglycerol lipase is recruited to presynapses and astroglia in aged human brain

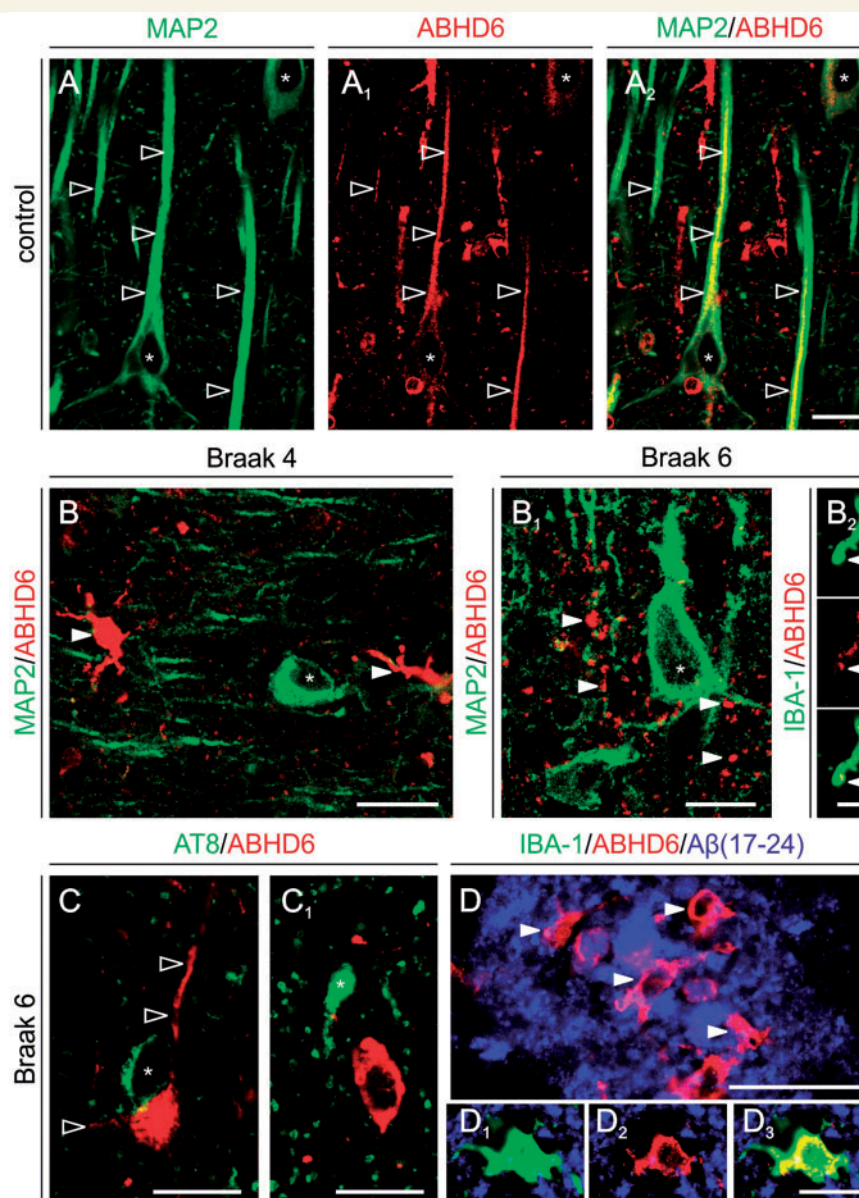
Although monoacylglycerol lipase has many substrates (Nomura *et al.*, 2010), it is considered to be the major enzyme inactivating > 80% of 2-arachidonoyl glycerol in adult rodent

brain (Blankman *et al.*, 2007). Chronic CB<sub>1</sub> cannabinoid receptor desensitization due to increased 2-arachidonoyl glycerol, but not other bioactive lipid levels in monoacylglycerol lipase<sup>−/−</sup> mice, confirms that 2-arachidonoyl glycerol is primarily degraded by monoacylglycerol lipase in the nervous system (Schlosburg *et al.*, 2010). Monoacylglycerol lipase is localized to presynapses in rodent (Dinh *et al.*, 2002) and human brains (Ludanyi *et al.*, 2011). However, monoacylglycerol lipase expression and subcellular localization remain elusive during ageing and in Alzheimer's disease.

We found, by using two antibodies directed against non-overlapping monoacylglycerol lipase epitopes and validated in monoacylglycerol lipase<sup>−/−</sup> mice (Keimpema *et al.*, 2010; Supplementary Fig. 2), prominent monoacylglycerol lipase immunoreactivity at three sites in the aged human hippocampus: (i) the somatic region of dentate granule cells (Fig. 5A–B<sub>1</sub>) and CA1 pyramidal neurons (Fig. 5C); (ii) nerve endings concentrating in the stratum moleculare of the dentate fascia (Fig. 5B<sub>1</sub>) and the stratum radiatum of the Ammon's horn subfields (Fig. 5C); and (iii) astroglia-like cells randomly distributed across hippocampal laminae (Fig. 5B<sub>1</sub> and H). Somatic monoacylglycerol lipase immunoreactivity in pyramidal cells is primarily present in the cytosol (Fig. 5D–D<sub>3</sub>). Although moderate monoacylglycerol lipase immunoreactivity was occasionally seen in the proximal segment of apical dendrites, overall monoacylglycerol lipase is absent in the dendritic tree of principal neurons (Fig. 5C). Monoacylglycerol lipase ubiquitously coexists with CB<sub>1</sub> cannabinoid receptors in presynapse-like puncta apposing pyramidal cells' dendrites, suggesting that monoacylglycerol lipase retains its presynaptic localization in the aged human hippocampus (Fig. 5E–E<sub>3</sub>). We have confirmed our histochemical findings by 3D reconstruction of pyramidal cell dendrites and perisynaptic astroglia end-feet (Fig. 5F and F<sub>1</sub>) and found a complete lack of co-localization between monoacylglycerol lipase and MAP2, a somatodendritic marker of neurons (Peng *et al.*, 1986), as well as glial fibrillary acidic protein in astroglia.

Next, we asked whether monoacylglycerol lipase and CB<sub>1</sub> cannabinoid receptors coexist throughout the hippocampal parenchyma or are only recruited to synaptic terminal-like specializations apposing MAP2<sup>+</sup> somatodendritic elements. Quantitative immunofluorescence morphometry (Supplementary Fig. 6C) revealed moderate correlation between the intensities of monoacylglycerol lipase and CB<sub>1</sub> cannabinoid receptor immunoreactivities at sites of co-localization (Fig. 5G), suggesting that recruitment of the two markers to the same sites may proceed largely independently of one another. We found that the area occupancy of monoacylglycerol lipase immunoreactivity exceeds that of the CB<sub>1</sub> cannabinoid receptor (Fig. 5G<sub>1</sub>) implying differences between the axonal transport, overall expression levels or subcellular recruitment of monoacylglycerol lipase and CB<sub>1</sub> cannabinoid receptor in the aged human brain. Accordingly, we found that only  $12.6 \pm 1.2\%$  of monoacylglycerol lipase<sup>+</sup> structures are labelled for CB<sub>1</sub> cannabinoid receptors. In contrast,  $25.1 \pm 2.2\%$  of CB<sub>1</sub> cannabinoid receptor immunoreactivity co-localizes with that of monoacylglycerol lipase (Fig. 5G<sub>2</sub>). Thus, our data suggest that monoacylglycerol lipase can accumulate in CB<sub>1</sub> cannabinoid receptor<sup>+</sup> presynapses in the human hippocampus to terminate retrograde 2-arachidonoyl glycerol signalling.

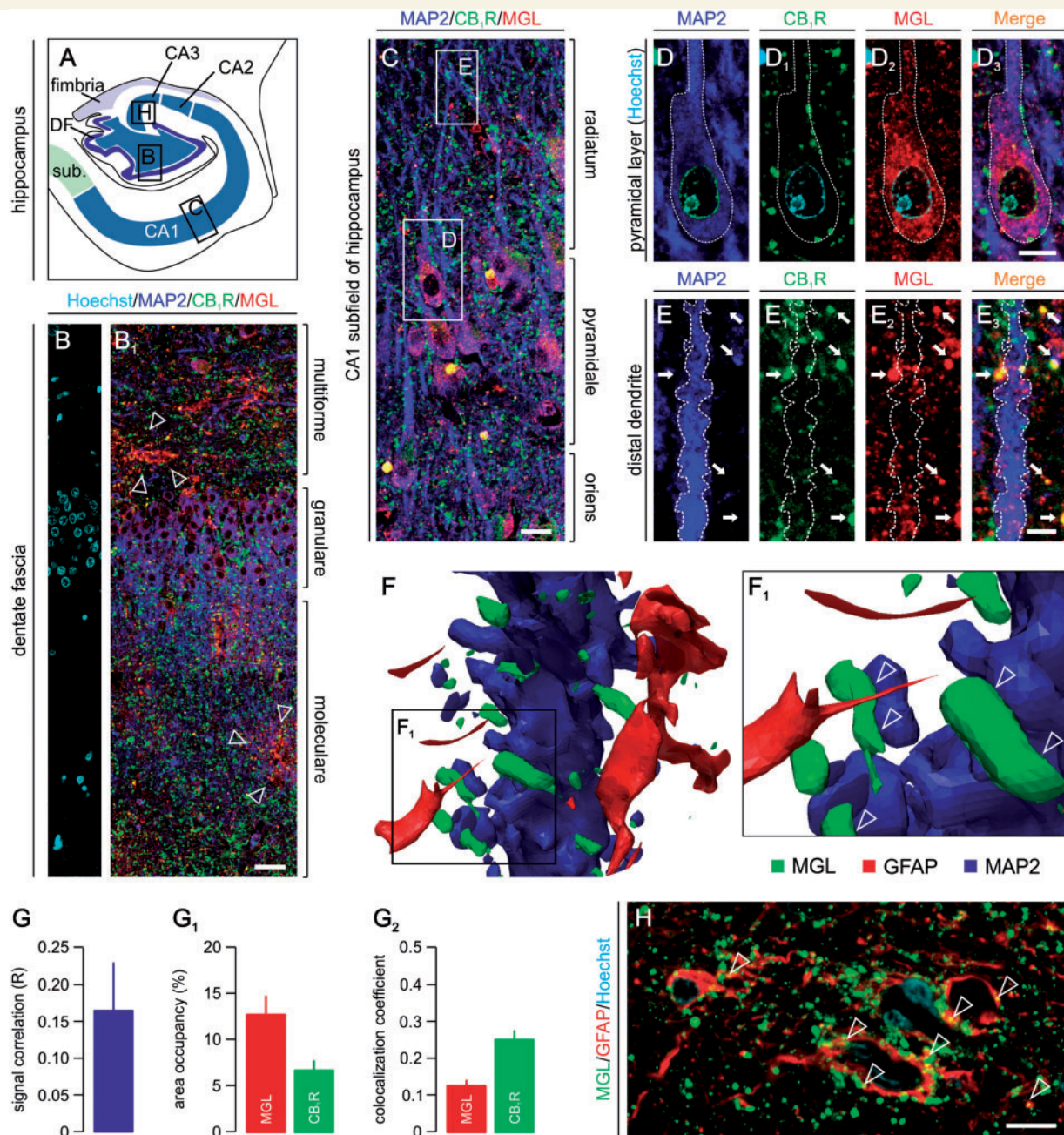




**Figure 4** Pathological alterations in the cellular distribution of serine hydrolase ABHD6 in Alzheimer's hippocampus. (A–A<sub>2</sub>) ABHD6 is distributed along the somatodendritic axis of hippocampal pyramidal cells in aged (control) human hippocampus. (B) We found ABHD6 expression in small, multipolar MAP2<sup>−</sup> cells, presumed microglia, coincident with a decrease in dendrite labelling in neurons (asterisk) in Braak 2–4 disease. (B<sub>1</sub> and B<sub>2</sub>) This Alzheimer-related ABHD6 distribution pattern is exacerbated in Braak 6 with ABHD6 immunoreactivity localized to small calibre, IBA1<sup>+</sup> microglia processes. (C and C<sub>1</sub>) ABHD6 is excluded from AT8<sup>+</sup> neurons (asterisk), though retained in proximal dendrites of cells without appreciable neurofibrillary pathology. (D–D<sub>3</sub>) ABHD6<sup>+</sup>/IBA1<sup>+</sup> microglia populate plaque-laden regions in severe Alzheimer's disease. Open and solid arrowheads point throughout to ABHD6<sup>+</sup> dendrites and microglia-like cells, respectively. Scale bars = 12 μm.

We used western analysis to compare monoacylglycerol lipase protein levels in Braak stage III/IV and Braak stage VI patients as well as age-matched controls, and found significantly increased levels of both major monoacylglycerol lipase isoforms in Braak stage VI hippocampi (Fig. 1A, F and F<sub>1</sub>). Correlation analysis substantiated a positive relationship between expression levels of the two major monoacylglycerol lipase isoforms (Fig. 1G). We have refined these results by verifying that advancing Braak stages in

Alzheimer's disease couple to gradually increased monoacylglycerol lipase levels in an isoform (Fig. 6A and A<sub>1</sub>) and post-mortem delay-independent manner (Fig. 6A<sub>2</sub>). Since we performed western analysis on total protein samples from human hippocampi, several unanswered questions remained including: (i) whether increased monoacylglycerol lipase concentrations represent novel expression sites as a result of ongoing neurodegeneration as well as neuroinflammation in Alzheimer's disease; (ii) whether defunct





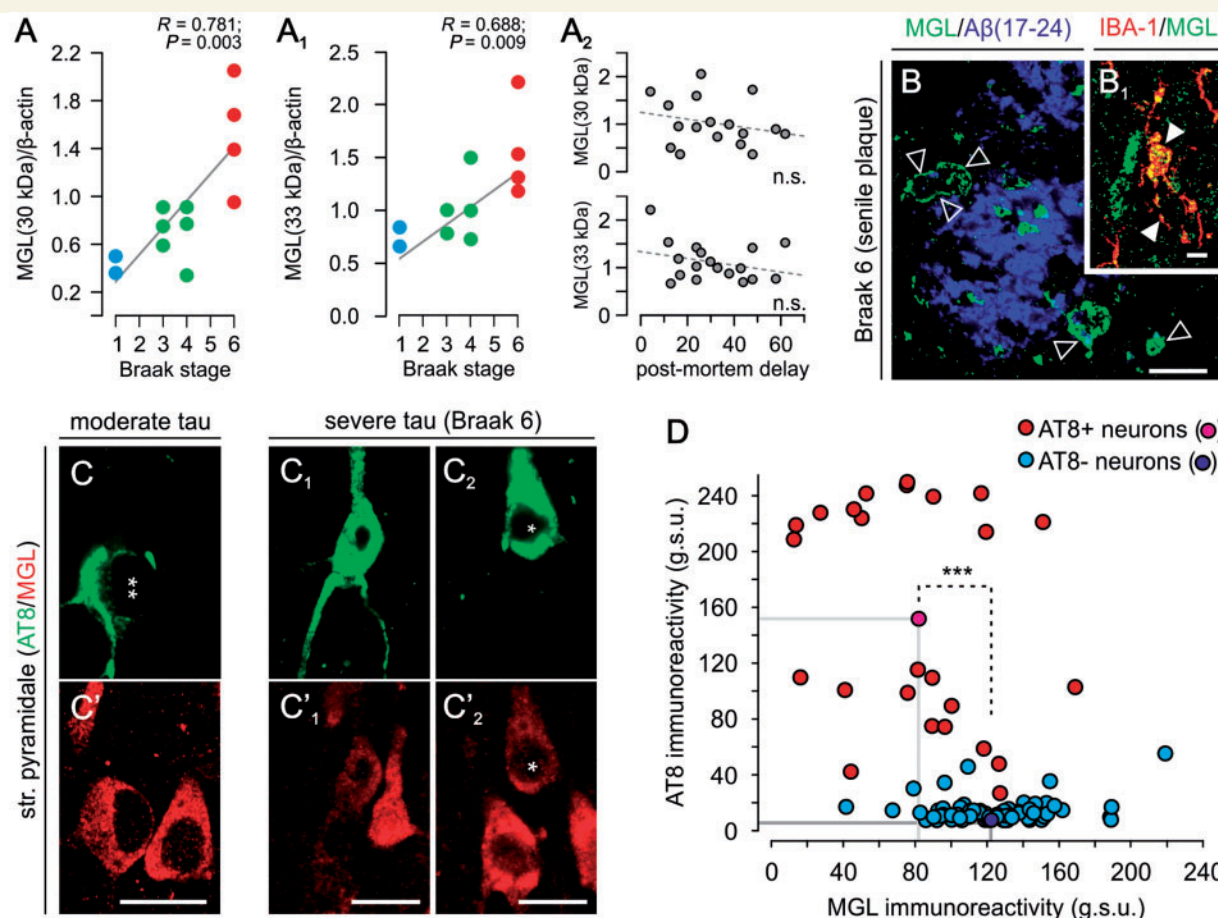


**Figure 6** Monoacylglycerol lipase localization in Alzheimer's hippocampus. (A and A<sub>1</sub>) Monoacylglycerol lipase (MGL) isoform expression exhibits positive correlation with Alzheimer's progression. (A<sub>2</sub>) This relationship is not biased by the post-mortem delay (h). (B and B<sub>1</sub>) IBA-1<sup>+</sup> microglia cells (arrowheads) recruited to senile amyloid plaques express monoacylglycerol lipase. (C–C<sub>2</sub>) Monoacylglycerol lipase expression is retained at reduced levels in neurons with moderate (C and double asterisk) and severe (C<sub>1</sub>, C<sub>2</sub> and single asterisk) neurofibrillary pathology. (D) Quantitative immunofluorescence analysis of monoacylglycerol lipase levels in neurons with (AT8<sup>+</sup>) or without (AT8<sup>-</sup>) hyperphosphorylated tau. Symbols in brackets denote group means. g.s.u. = grey-scale unit. \*\*\* $P < 0.001$  (Student's *t*-test). Scale bars = 12 μm (C'–C<sub>2</sub>'), 8 μm (B and B<sub>1</sub>).

neurons presenting cytoskeletal abnormalities, such as hyperphosphorylated tau, lose monoacylglycerol lipase expression as seen for ABHD6; and (iii) whether Alzheimer's disease impacts the metabolic competence of monoacylglycerol lipase by impairing its recruitment to the plasmalemma.

In the Alzheimer's hippocampus, we find that monoacylglycerol lipase<sup>+</sup>/IBA-1<sup>+</sup> microglia cells accumulate around senile plaques (Fig. 6B and B<sub>1</sub>). Although quantitative morphometry was not an objective of the present report, a clear increase in the density of monoacylglycerol lipase<sup>+</sup> microglia can be seen when comparing Braak stage III/IV versus Braak stage VI brains. Hippocampal principal cells—both pyramidal cells of the Ammon's horn subfields and dentate granule cells—express monoacylglycerol lipase. We found that AT8<sup>+</sup> pyramidal cells retain monoacylglycerol lipase expression (Fig. 6C–C<sub>2</sub>'), although at significantly lower levels than those without intracellular tau pathology [Fig. 6D;  $121.85 \pm 3.73$  grey scale unit (AT8<sup>-</sup> neurons) versus  $81.75 \pm 8.31$  grey scale unit (AT8<sup>+</sup> neurons);  $P < 0.001$ ]. Our data

cumulatively indicate that both microglia (Fig. 6B) and astroglia (Fig. 5H) can serve as sources of monoacylglycerol lipase, and a progressive shift of monoacylglycerol lipase expression from damaged neurons to activated micro- and astroglia occurs in Alzheimer's disease.

## Gene expression profiling in mouse microglia

Activated microglia have previously been shown to express CB<sub>2</sub> cannabinoid receptors in Alzheimer's disease (Benito *et al.*, 2003; Ramirez *et al.*, 2005) and Down's syndrome (Nunez *et al.*, 2008), and pharmacological challenges can increase 2-arachidonoyl glycerol production in this cell type (Walter *et al.*, 2003). However, coexistence of molecular components determining an operational 2-arachidonoyl glycerol signalling network in activated microglia (i.e. CB/CB<sub>2</sub> cannabinoid receptors, DAGLs, ABHD6 and



monoacylglycerol lipase) capable to sustain autocrine and/or paracrine 2-arachidonoyl glycerol signalling remains unknown. We performed Affymetrix gene expression profiling coupled to quantitative polymerase chain reaction analysis (Fig. 7A) to test the expression of CB<sub>1</sub> cannabinoid receptors, CB<sub>2</sub> cannabinoid receptors, as well as 2-arachidonoyl glycerol metabolic enzymes in primary mouse microglia under experimental conditions mimicking pro-inflammatory transformation in Alzheimer's brains (Halleskog *et al.*, 2011). Under control conditions, CB<sub>1</sub> cannabinoid receptor, CB<sub>2</sub> cannabinoid receptor, DAGL $\alpha$ , DAGL $\beta$ , monoacylglycerol lipase, ABHD6 and ABHD12 expression levels exceeded the detection minimum of Affymetrix chips (data not shown). Microglia activation can proceed through amyloid- $\beta$ -independent mechanisms *in vivo* (Halleskog *et al.*, 2011). Therefore, we applied WNT-3A (300 ng/ml) to induce pro-inflammatory transformation of primary mouse microglia. WNT-3A significantly increased messenger RNA transcript levels of interleukin 6 and tumour necrosis factor  $\alpha$ , pro-inflammatory cytokines, relative to controls (Halleskog *et al.*, 2011). Simultaneously, WNT-3A reduced CB<sub>2</sub> cannabinoid receptor, DAGL $\alpha$  and DAGL $\beta$  messenger RNA expression, while leaving CB<sub>1</sub> cannabinoid receptor, monoacylglycerol lipase and ABHD6/12 expression unchanged (Fig. 7A). Quantitative polymerase chain reaction analysis of N13 microglia-like cells exposed to fibrillar amyloid- $\beta_{1-40}$  (100 nM versus non-treated controls), known to activate microglia (Ramirez *et al.*, 2005), showed significantly decreased messenger RNA transcript levels of CB<sub>1</sub> cannabinoid receptors ( $-61.3 \pm 3.1\%$  of control;  $n = 4/\text{condition}$ ;  $P = 0.017$ ) and DAGL $\alpha$  ( $-35.2 \pm 6.1\%$  of control;  $n = 3-4/\text{condition}$ ;  $P = 0.042$ ) but not of other molecular components of 2-arachidonoyl glycerol signalling (CB<sub>2</sub> cannabinoid receptor:  $-11.6 \pm 16.7\%$ ,  $P > 0.1$ ,  $n = 4/\text{condition}$ ; monoacylglycerol lipase:  $-60.3 \pm 4.4\%$ ;  $P > 0.1$ ,  $n = 3/\text{condition}$ ; Fig. 7A). In sum, these data demonstrate that microglia can express receptor and enzyme components of 2-arachidonoyl glycerol signalling networks, and respond to pro-inflammatory stimuli by transcriptional regulation of rate-limiting molecular constituents of 2-arachidonoyl glycerol signalling.

## 2-Arachidonoyl glycerol hydrolysing activity in Alzheimer's disease and on exposure to amyloid- $\beta$

Rearrangements in 2-arachidonoyl glycerol signalling networks may ultimately amplify Alzheimer-related synaptic impairment if subcellular enzyme redistribution is associated with impaired enzymatic activity. Acute amyloid- $\beta$  infusion in the rodent hippocampus increases 2-arachidonoyl glycerol concentrations, a finding that has been interpreted as an endogenous neuroprotective mechanism against amyloid- $\beta$ -induced oxidative stress (van der Stelt *et al.*, 2006). Here, we have tested the alternative hypothesis that amyloid- $\beta$ -induced increase in 2-arachidonoyl glycerol levels reflects impaired 2-arachidonoyl glycerol catabolism under disease conditions. We have focused on monoacylglycerol lipase as a candidate whose recruitment from the cytosol to its metabolically favoured position in the internal leaflet of the plasmalemma (Labar *et al.*, 2010) may be impeded by amyloid- $\beta$ -induced oxidative

damage to biological membranes in Alzheimer's disease (Ramirez *et al.*, 2005; Querfurth and LaFerla, 2010).

We measured the rate of 2-arachidonoyl glycerol degradation in frontal cortices of patients with Alzheimer's disease and age-matched controls by determining the amount of [1,2,3-<sup>3</sup>H]glycerol after incubating membrane or cytosol fractions with [<sup>3</sup>H]2-arachidonoyl glycerol. Membrane-associated 2-arachidonoyl glycerol hydrolysis significantly decreased in subjects with Alzheimer's disease, as compared with controls (28% of control,  $P < 0.05$ ; Fig. 7B). In turn, 2-arachidonoyl glycerol-degrading capacity in the cytosol increased proportionally in Alzheimer's brains (65% of control,  $P < 0.05$ ; Fig. 7B), suggesting the subcellular redistribution of 2-arachidonoyl glycerol-degrading enzymes in human brain [total activity:  $2468 \pm 96$  (control) versus  $2391 \pm 122$  (Alzheimer) picomole 2-arachidonoyl glycerol-degraded/mg protein/15 min;  $P = 0.635$ ,  $n = 9/\text{group}$ ]. Multiple enzymes, including monoacylglycerol lipase, ABHD6 and FAAH, contribute to 2-arachidonoyl glycerol degradation in the adult brain (Blankman *et al.*, 2007). To assess monoacylglycerol lipase's specific role in altered 2-arachidonoyl glycerol hydrolysis in Alzheimer's disease, we measured the rate of [<sup>3</sup>H]2-arachidonoyl glycerol degradation in the presence of the monoacylglycerol lipase inhibitors, JZL184 (5  $\mu\text{M}$ ; Fig. 7C and C<sub>1</sub>) (Long *et al.*, 2009) or URB602 (1 mM; Supplementary Fig. 9) (King *et al.*, 2007). We found that JZL184 inhibits 50.2% of 2-arachidonoyl glycerol hydrolysis in membranes prepared from control brains ( $P < 0.01$ ; Fig. 7C). In contrast, JZL184 inhibits only 29.6% ( $P < 0.05$ ) of cytosolic 2-arachidonoyl glycerol hydrolysis in control human-cortical homogenates (Fig. 7C<sub>1</sub>). In membrane preparations from Alzheimer's brains (Fig. 7C), 11.6% of 2-arachidonoyl glycerol hydrolysis activity is eliminated by JZL184, coincident with a significant reduction of membrane-associated monoacylglycerol lipase protein levels in the cerebral cortex of subjects with Alzheimer's disease (Supplementary Fig. 8A–A<sub>2</sub>). Conversely, surplus 2-arachidonoyl glycerol hydrolysis activity in cytosol fractions of Alzheimer's brains is JZL184 sensitive (32.0%;  $P < 0.01$  versus vehicle-treated controls; Fig. 7C<sub>1</sub>). URB602 exhibited a similar pharmacological profile (Supplementary Fig. 8B and B<sub>1</sub>). We excluded the contribution of FAAH to 2-arachidonoyl glycerol degradation by showing negligible ( $\leq 10\%$ ) inhibition by URB597, a potent FAAH inhibitor (Mor *et al.*, 2004) (see also Supplementary Fig. 8C). These data suggest that (i) monoacylglycerol lipase selectively undergoes subcellular redistribution; (ii) the contribution of JZL184/URB602-insensitive enzymes to 2-arachidonoyl glycerol degradation (e.g. ABHD6 in microglia, Fig. 4B<sub>1</sub>) increases in Alzheimer's disease; and (iii) FAAH—whose activity is decreased in Alzheimer's disease (Supplementary Fig. 8C)—does not contribute focally to 2-arachidonoyl glycerol hydrolysis in human brain.

Next, we hypothesized that amyloid- $\beta$  may impact the activity of enzymes involved in 2-arachidonoyl glycerol hydrolysis. Therefore, membrane and cytosol fractions from control brains were acutely exposed to amyloid- $\beta_{1-40}$  at 1  $\mu\text{M}$  final concentration. Pre-incubation with amyloid- $\beta_{1-40}$  for 10 min increased 2-arachidonoyl glycerol catabolism in both membrane and cytosol fractions of human cortices [membrane:  $2118 \pm 73$  (control;  $n = 9$ ) versus  $2398 \pm 109$  (amyloid- $\beta_{1-40}$ ;  $n = 8$ ),  $P = 0.045$ ;

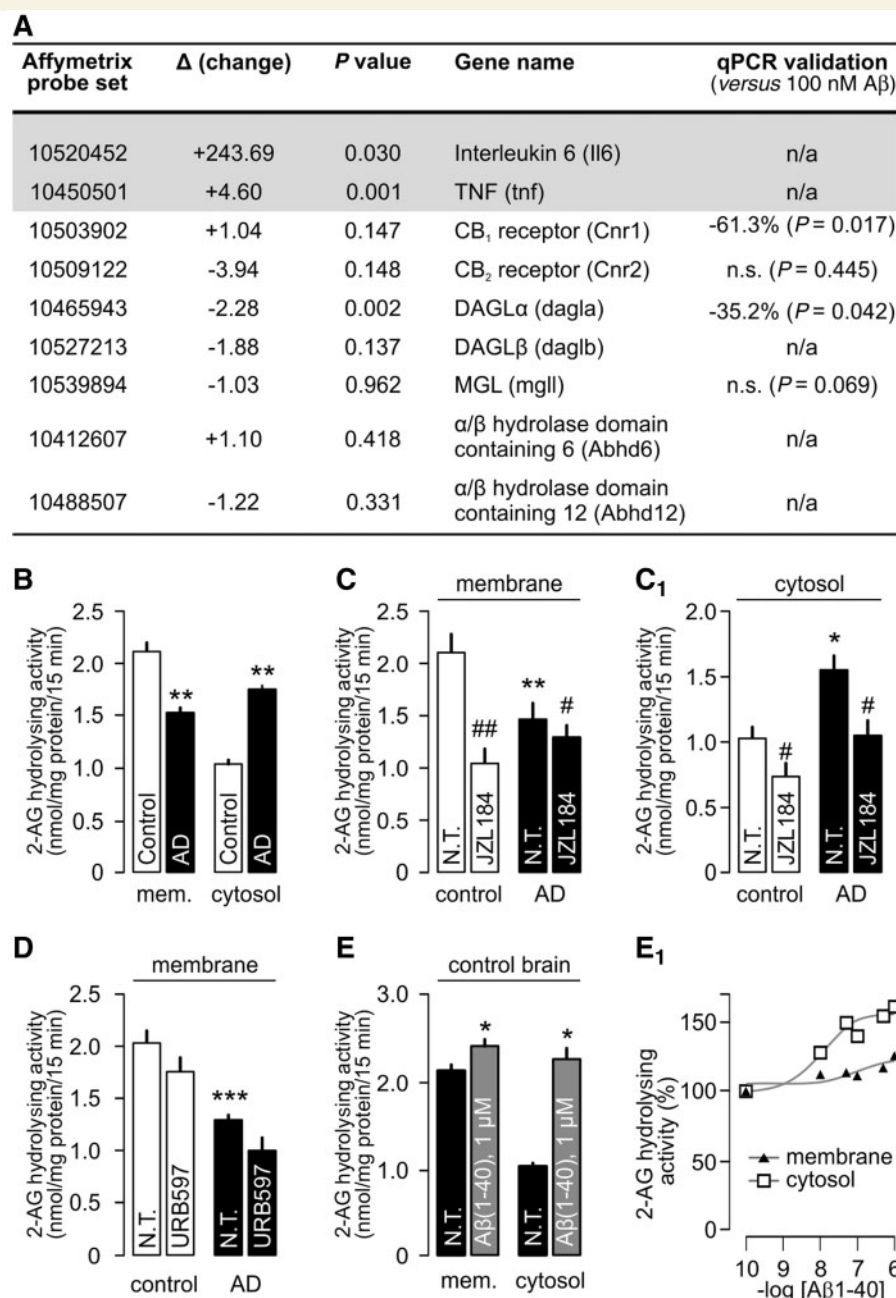


**Figure 7** 2-Arachidonoyl glycerol degradation in Alzheimer's disease and its amyloid- $\beta_{1-40}$ -induced activation. **(A)** Pro-inflammatory transformation by WNT-3A (300 ng/ml, 6 h) (Halleskog *et al.*, 2011) down-regulates monoacylglycerol lipase (MGL) expression in primary mouse microglia. Interleukin-6 and tumour necrosis factor (TNF) were used as positive (internal) controls. **(B)** 2-Arachidonoyl glycerol is differentially metabolized in the frontal cortex in Alzheimer's disease: Membrane-associated 2-arachidonoyl glycerol-degrading enzymatic activity is decreased, while cytosolic 2-arachidonoyl glycerol-degrading activity is significantly increased, relative to controls. **(C)** Membrane-associated monoacylglycerol lipase activity accounts for ~60% of total 2-arachidonoyl glycerol hydrolysis activity as revealed by JZL184 application (Supplementary Fig. 8B and B<sub>1</sub>) in membrane samples prepared from control human specimens. Note that JZL184-sensitive 2-arachidonoyl glycerol-degrading activities are selectively lost in Alzheimer's disease. **(C<sub>1</sub>)** 2-Arachidonoyl glycerol hydrolysis activity significantly increases in cytosol fractions from Alzheimer's brains, as compared to controls. JZL184 partially reduces 2-arachidonoyl glycerol degradation in cytosolic fractions prepared from control brains and eliminates disease-associated enhancement of 2-arachidonoyl glycerol catabolism in Alzheimer's brains (AD). **(D)** FAAH does not contribute to 2-arachidonoyl glycerol degradation at either subcellular fraction as tested by URB597. **(E)** Pre-incubation of cortical tissue homogenates from control subjects with amyloid- $\beta_{1-40}$  (A $\beta_{1-40}$ ) significantly increases both membrane-bound and cytosolic 2-arachidonoyl glycerol metabolism. **(E<sub>1</sub>)** Amyloid- $\beta_{1-40}$  induces 2-arachidonoyl glycerol-degrading enzymatic activity in a dose-dependent manner. \* $P < 0.05$ , \*\* $P < 0.01$  versus controls; \*\*\* $P < 0.05$ , \*\*\*\* $P < 0.01$  versus non-treated samples. n/a = not analysed; NS = not significant; NT = non-treated; qPCR = quantitative polymerase chain reaction.

cytosol:  $1038 \pm 41$  (control;  $n = 9$ ) versus  $2265 \pm 112$  (amyloid- $\beta_{1-40}$ ;  $n = 9$ ),  $P < 0.01$ ; picomole 2-arachidonoyl glycerol-degraded/mg protein/15 min; Fig. 7E] in a shallow dose-dependent fashion (Fig. 7E<sub>1</sub>), thus mimicking changes in 2-arachidonoyl glycerol hydrolysing activity in Alzheimer's brains. We found that nM amyloid- $\beta_{1-40}$  concentrations of likely pathophysiological significance (Walsh *et al.*, 2002) can augment 2-arachidonoyl glycerol degradation (Fig. 7E<sub>1</sub>). Thus, we conclude that amyloid- $\beta$  contributes to the control of 2-arachidonoyl glycerol catabolism in the human brain and reduces monoacylglycerol lipase's 2-arachidonoyl glycerol hydrolytic capacity in membrane fractions otherwise required to inactivate 2-arachidonoyl glycerol during retrograde synaptic signalling.

## Amyloid- $\beta$ prolongs depolarization-induced suppression of inhibition

Monoacylglycerol lipase removal from the plasma membrane could increase the duration of signalling-competent 2-arachidonoyl glycerol availability following its release from postsynaptic neurons, and prolong depolarization-induced suppression of inhibition (Kano *et al.*, 2009). Consequently, enhanced 2-arachidonoyl glycerol signalling could disrupt the balance between inhibitory and excitatory neurotransmission. A causal relationship between high focal amyloid- $\beta$  concentration and errant 2-arachidonoyl glycerol signalling may be particularly appealing to further the mechanistic concept linking synaptic impairment to neuronal hyper excitability (Busche *et al.*, 2008; Minkeviciene *et al.*, 2009) and excitotoxic neuronal damage (Mattson and Chan, 2003).

Transgenic mouse models generating age-dependent amyloid- $\beta$  burden in the cerebral cortex and hippocampus, e.g. APdE9 mice (Jankowsky *et al.*, 2004), are popular to study molecular pathomechanisms of Alzheimer's disease. However, biochemical protein profiling suggests that APdE9 mice might be inappropriate to recapitulate molecular underpinnings of disrupted 2-arachidonoyl glycerol signalling in Alzheimer's disease (Supplementary Fig. 9). Therefore, we tested whether bath-applied amyloid- $\beta_{1-42}$  could acutely evoke Alzheimer-related subcellular rearrangements in the molecular architecture of 2-arachidonoyl glycerol signalling networks. We show that non-fibrillar amyloid- $\beta_{1-42}$ —dissolved freshly in the superfusate (Minkeviciene *et al.*, 2009)—facilitates CB<sub>1</sub> cannabinoid receptor removal from the cytosol ( $89.87 \pm 2.29\%$  of control;  $n = 5$ ,  $P = 0.002$ ; Fig. 8A and A<sub>1</sub>) and enrichment in membrane fractions ( $123.13 \pm 13.26\%$  of control) prepared from hippocampi of juvenile wild-type mice. Subcellular DAGL $\alpha$  distribution appeared stochastic with a trend towards cytosolic enrichment ( $119.76 \pm 14.59\%$ ;  $n = 5$ /condition,  $P > 0.1$ ; membrane fraction:  $77.48 \pm 11.15\%$ ;  $n = 5$ /condition,  $P = 0.052$ ; Fig. 8A and A<sub>2</sub>). Amyloid- $\beta_{1-42}$  arrested monoacylglycerol lipase in the cytosol ( $149.16 \pm 14.59\%$  of control;  $n = 6$ /group,  $P = 0.003$ ), while leaving membrane-associated monoacylglycerol lipase unchanged ( $97.95 \pm 14.60\%$  control;  $P > 0.8$ ; Fig. 8A and A<sub>3</sub>) in 1 h. We hypothesized that the amyloid- $\beta_{1-42}$ -induced enhanced cell-surface availability of the CB<sub>1</sub> cannabinoid receptor would alter 2-arachidonoyl glycerol signalling. Therefore, we sought to determine whether amyloid- $\beta_{1-42}$  augments the 2-arachidonoyl

glycerol-mediated suppression of inhibitory neurotransmission in the hippocampus. We studied depolarization-induced suppression of inhibition at inhibitory synapses because amyloid- $\beta_{1-42}$  accumulation in senile plaques has been shown to impair GABA neurotransmission, thus provoking focal neuronal hyper excitability in a transgenic model of Alzheimer's disease (Busche *et al.*, 2008).

Using whole-cell patch recording of Ammon's horn 1 subfield hippocampal neurons in brain slices prepared from juvenile mice, we elicited a baseline depolarization-induced suppression of inhibition by briefly depolarizing (1 s, from  $-80$  to  $0$  mV) the pyramidal cell (Fig. 8B). Depolarization-induced suppression of inhibition was detected in all control cells, had a maximal magnitude of  $25.7 \pm 3.1\%$  when measured between 1 and 5 s after postsynaptic cell depolarization and normalized to the pre-depolarization baseline ( $n = 9$ ). The decay time constant ( $\tau$ ) of depolarization-induced suppression of inhibition was  $9.15 \pm 1.39$  (s). Bath application of amyloid- $\beta_{1-42}$  for 1 h did not significantly affect maximal synaptic depression in pyramidal cells (depolarization-induced suppression of inhibition magnitude:  $32.9 \pm 4.4\%$ ,  $n = 10$ ,  $P = 0.233$  versus control; Fig. 8B<sub>1</sub> and B<sub>2</sub>). Nevertheless, the magnitude of synaptic depression on non-fibrillar amyloid- $\beta_{1-42}$  pre-treatment was significantly different from that in control cells from 5–15 s post-stimulus [5 s:  $32.5 \pm 5.1\%$  (amyloid- $\beta$ ) versus  $18.0 \pm 5.1\%$  (control),  $P = 0.039$ ; 10 s:  $27.4 \pm 4.3\%$  (amyloid- $\beta$ ) versus  $8.8 \pm 0.4\%$  (control),  $P = 0.004$ ; 15 s:  $19.4 \pm 5.7\%$  (amyloid- $\beta$ ) versus  $4.5 \pm 4.7\%$  (control),  $P = 0.047$ ]. Non-fibrillar amyloid- $\beta_{1-42}$  prolonged depolarization-induced suppression of inhibition, as indicated by a significant increase in its mean decay time constant [ $\tau = 43.69 \pm 11.99$  (s),  $n = 10$ ,  $P = 0.018$  versus control]. We used AM251 ( $1 \mu\text{M}$ ) to verify that depolarization-induced suppression of inhibition was dependent on CB<sub>1</sub> cannabinoid receptor activation (Fig. 8C, Supplementary Fig. 10A and A<sub>1</sub>). AM251 completely abolished depolarization-induced suppression of inhibition in all cases tested. Next, we sought to determine whether the amyloid- $\beta$ -induced enhancement of depolarization-induced suppression of inhibition is exclusively due to CB<sub>1</sub> cannabinoid receptor activation or if amyloid- $\beta$  uncovers a secondary mechanism operating at hippocampal synapses otherwise sensitive to AM251. We found that amyloid- $\beta_{1-42}$  does not induce significant depolarization-induced suppression of inhibition in the presence of AM251 (Fig. 8D and D<sub>1</sub>). Cumulatively, our data imply that amyloid- $\beta$  prolongs 2-arachidonoyl glycerol signalling, which will impair GABAergic transmission, thus likely contributing to the progressive development of synaptic failure in Alzheimer's disease.

## Discussion

This report describes significant changes to (i) the molecular architecture; (ii) cellular identity; and (iii) function of 2-arachidonoyl glycerol metabolism in defined patient cohorts with clinicopathologically-verified Alzheimer's disease, as well as in transgenic mice and acute pharmacological models of Alzheimer's-like neuronal dysfunction. Although we cannot entirely rule out altered signal transduction downstream from CB<sub>1</sub> cannabinoid receptors (Lee *et al.*, 2010), our biochemical and histochemical findings



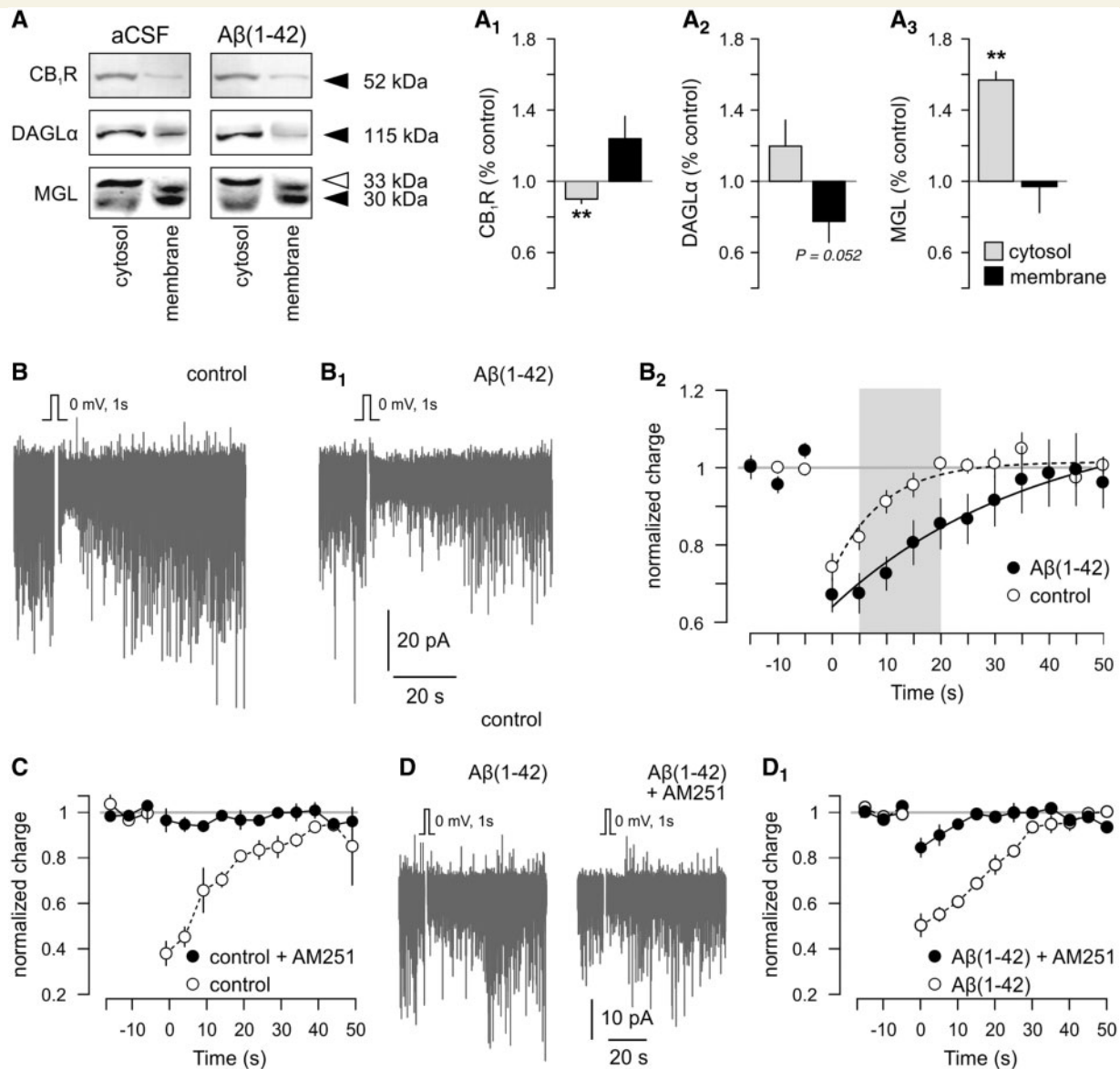


**Figure 8** Amyloid- $\beta_{1-42}$  triggers subcellular redistribution of 2-arachidonoyl glycerol signalling networks and prolongs depolarization-induced suppression of inhibition. (**A**–**A**<sub>3</sub>) Representative images of molecular targets resolved by Western blotting. Cytosol and membrane fractions are from the same sample to establish the impact of amyloid- $\beta_{1-42}$  on subcellular receptor and enzyme recruitment, as compared to controls in artificial cerebrospinal fluid (aCSF). Amyloid- $\beta_{1-42}$  [(Aβ(1-42))] exposure significantly alters intracellular versus cell surface concentrations of CB<sub>1</sub> cannabinoid receptors (**A**<sub>1</sub>), DAGLα (**A**<sub>2</sub>) and monoacylglycerol lipase (**A**<sub>3</sub>). Data on monoacylglycerol lipase (MGL) show cumulative changes in this enzyme's 33 and 30 kDa isoforms. (**B**) Representative experiment showing depolarization-induced suppression of inhibition induced by a step depolarization of an Ammon's horn 1 pyramidal neuron. (**B**<sub>1</sub>) Postsynaptic depolarization-induced reduction of spontaneous inhibitory postsynaptic currents (downward deflection from baseline) is prolonged by bath-applied amyloid- $\beta_{1-42}$  (1  $\mu$ M). (**B**<sub>2</sub>) Summary of depolarization-induced suppression of inhibition magnitude and kinetics measured in control (open circles;  $n = 10$  cells) or in the presence of amyloid- $\beta_{1-42}$  (solid circles;  $n = 11$ ). AM251 (1  $\mu$ M) abolishes depolarization-induced suppression of inhibition in control (**C**), as well as amyloid- $\beta_{1-42}$ -superfused Ammon's horn 1 pyramidal neurons (**D** and **D**<sub>1</sub>). \*\* $P < 0.01$  (Student's  $t$ -test). Data were expressed as means  $\pm$  SEM.

cumulatively highlight that 2-arachidonoyl glycerol signalling in neurons is primarily impaired at the level of metabolic enzymatic control of ligand availability in Alzheimer's disease. We also propose that activated microglia, accumulating in Alzheimer's brains and contributing to chronic neuroinflammation, have a

fundamental role in modifying 2-arachidonoyl glycerol signalling, particularly in amyloid- $\beta$ -laden brain microdomains around senile plaques, and might impact synaptic communication.

A separate series of experiments were directed towards exploring whether Alzheimer's pathology alters the levels of NAPE-PLD

and FAAH, implicated in anandamide metabolism (Cravatt *et al.*, 1996; Ueda *et al.*, 2005), or the function of TRPV<sub>1</sub> receptors (Kofalvi *et al.*, 2007), binding anandamide but not 2-arachidonoyl glycerol. We failed to detect Alzheimer's-related changes in either NAPE-PLD, FAAH, TRPV<sub>1</sub> protein levels (Supplementary Fig. 5A–F<sub>2</sub>) or [<sup>3</sup>H]resiniferatoxin binding at TRPV<sub>1</sub> receptors (Fig. 5G<sub>2</sub>). However, interpretation of our data may be curtailed by several factors including the relative paucity of information on (i) the availability of essential phospholipid precursors in Alzheimer's disease; (ii) the relative contribution of enzymes other than NAPE-PLD to anandamide biosynthesis (Simon and Cravatt, 2008); and (iii) the mechanistic contribution of TRPV<sub>1</sub> receptors to memory retention deficits (Micale *et al.*, 2010). Therefore, Alzheimer's-related changes to anandamide bioavailability and synaptic actions cannot be excluded.

## Trans-synaptic 2-arachidonoyl glycerol signalling in Alzheimer's disease

Endocannabinoids and phytocannabinoids are recognized to exert profound neuroprotection in models of peripheral nerve injury (Yoles *et al.*, 1996), excitotoxicity (Khaspekov *et al.*, 2004) and neurodegeneration (Ludanyi *et al.*, 2008; Palazuelos *et al.*, 2009; Blazquez *et al.*, 2011) through CB<sub>1</sub> cannabinoid receptor/CB<sub>2</sub> cannabinoid receptor-dependent (Palazuelos *et al.*, 2009) or -independent mechanisms (Lastres-Becker *et al.*, 2005).

In microlesion models of Alzheimer's disease, amyloid- $\beta_{1-42}$  infusion in the rat cerebral cortex significantly increases 2-arachidonoyl glycerol but not anandamide levels in the hippocampus (van der Stelt *et al.*, 2006). This amyloid- $\beta_{1-42}$ -induced elevation of 2-arachidonoyl glycerol concentrations is further augmented by inhibiting endocannabinoid reuptake to reverse hippocampal neuronal damage and decrease glial activation, thus preventing the loss of memory retention (van der Stelt *et al.*, 2006). Our data are significant as they corroborate and notably extend the above observations by providing insights into specific Alzheimer's-associated molecular rearrangements of 2-arachidonoyl glycerol metabolism. We suggest that both reactive astrocytes (Scuderi *et al.*, 2011) and microglia can participate in enhanced 2-arachidonoyl glycerol biosynthesis around amyloid- $\beta$ -rich foci in the Alzheimer's brain. In contrast, 2-arachidonoyl glycerol-degrading capacity in neurons could be substantially reduced if ABHD6 and monoacylglycerol lipase expressions are significantly suppressed in injured neurons with neurofibrillary pathology. Therefore, the net contribution of 2-arachidonoyl glycerol signalling to suppress pre-synaptic neurotransmitter release may be significantly increased. In fact, *ex vivo* experiments recapitulate the above scenario of amyloid- $\beta$ -induced synaptic impairment by showing prolonged depolarization-induced suppression of inhibition at inhibitory afferents of Ammon's horn 1 subfield pyramidal cells. Amyloid- $\beta$ -induced enhancement of depolarization-induced suppression of inhibition is also important to reconcile previous findings that have suggested both pre- and postsynaptic sites of action for amyloid- $\beta$  when disrupting spike timing-dependent plasticity at cortical synapses (Shemer *et al.*, 2006).

Postsynaptic NMDA and AMPA receptors are widely viewed as key molecular targets of amyloid- $\beta$  to disrupt synaptic plasticity (Kamenetz *et al.*, 2003; Snyder *et al.*, 2005; Shemer *et al.*, 2006). In particular, amyloid- $\beta$ -induced impairment of NMDA/AMPA receptor trafficking at the postsynapse can disrupt Ca<sup>2+</sup> signalling in dendritic spines targeted by excitatory afferents (Snyder *et al.*, 2005). DAGLs accumulate at the neck of dendritic spines (Yoshida *et al.*, 2006) where they are anchored by homer-1 and -2 family scaffolding proteins (Jung *et al.*, 2007; Rolloff *et al.*, 2010). Notably, soluble amyloid- $\beta$  oligomers induce the disassembly of homer-containing postsynaptic clusters (Roselli *et al.*, 2009), thus potentially affecting the subcellular recruitment and signalling competence of DAGLs. These changes, together with increased DAGL activity upon amyloid- $\beta$ -induced Ca<sup>2+</sup> overload in neurons (provided that DAGLs are Ca<sup>2+</sup>-dependent) (Bisogno *et al.*, 2003) and increased DAGL expression in microglia can significantly increase 2-arachidonoyl glycerol availability in Alzheimer's disease.

Alzheimer's disease has long been viewed as a disease stemming from neuronal hypofunction. This concept has recently been challenged by demonstrating that neurons near amyloid- $\beta$ -containing plaques are focally 'hyperactive', while others away from plaque-laden areas are silent (Busche *et al.*, 2008). Neuronal hyperactivity is suggested to be due to a relative decrease in synaptic inhibition (Busche *et al.*, 2008). We found that the molecular composition of 2-arachidonoyl glycerol signalling networks undergoes profound modifications around amyloid- $\beta$ -containing senile plaques in the human hippocampus in Alzheimer's disease. These observations led us to hypothesize that if the efficacy of retrograde signalling is increased in Alzheimer's disease then it might contribute to synapse silencing.

Our proof-of-concept neurophysiology experiments support this notion by showing a significant increase in depolarization-induced suppression of inhibition duration, thus suggesting that 2-arachidonoyl glycerol-mediated feedback may be a particular mechanism through which amyloid- $\beta$  could disrupt inhibitory neurotransmission. Functionally, depolarization-induced suppression of inhibition may serve to lengthen the firing duration of postsynaptic neurons by abating inhibitory inputs during periods of high excitatory activity. By prolonging depolarization-induced suppression of inhibition decay, amyloid- $\beta$  may further extend the excitatory neurons' firing periods, thus increasing overall network excitability. Previously, we have reported (Minkeviciene *et al.*, 2009) that amyloid- $\beta$  induces neuronal hyper-excitability by significantly depolarizing the resting membrane potential of excitatory neurons and lowering their response threshold. This effect is exerted without a requirement for preceding postsynaptic activation, as in the case with depolarization-induced suppression of inhibition. Thus, prolonging depolarization-induced suppression of inhibition decay by reorganizing endocannabinoid signalling is a potential mechanism by which amyloid- $\beta$  can modulate neuronal network excitability. Since inhibitory synapses are more resistant to Alzheimer's disease than excitatory ones (Bell *et al.*, 2006), prolonged depolarization-induced suppression of inhibition may destabilize hippocampal networks by shifting the net balance of inhibition and excitation in favour of excitation. Thus, decreased inhibitory neurotransmission will ultimately manifest in

'hyperactivity' (Busche *et al.*, 2008; Minkeviciene *et al.*, 2009), which may explain the increased incidence of unprovoked epileptic seizures in patients with Alzheimer's disease (Hauser *et al.*, 1986).

Synaptic impairment is a central feature of Alzheimer-related cognitive decline. It is widely accepted that amyloid- $\beta$  preferentially targets excitatory synapses (Lacor *et al.*, 2004). CB<sub>1</sub> cannabinoid receptors are expressed by both inhibitory interneurons and pyramidal cells with inhibitory terminals containing exceptionally high levels of this receptor (Kawamura *et al.*, 2006). Our finding that CB<sub>1</sub> cannabinoid receptor levels fail to correlate with pre-synaptic markers suggests that the molecular changes in 2-arachidonoyl glycerol signalling networks we have identified are unlikely to reflect the overall rate of synaptic demise in moderate or severe Alzheimer's disease. Even if amyloid- $\beta$  induces opposing—and proportional—changes in CB<sub>1</sub> cannabinoid receptor expression (that is, to increase CB<sub>1</sub> cannabinoid receptor content in inhibitory but decrease CB<sub>1</sub> cannabinoid receptor levels in excitatory terminals), the neurochemical homogeneity of perisomatic inhibitory synapses under endocannabinoid control (Kano *et al.*, 2009) suggests that amyloid- $\beta$  can impose functional modifications to endocannabinoid signalling at specific synapse populations. This concept is supported by the fact that acute amyloid- $\beta$  superfusion is unlikely to eliminate hippocampal synapses within the brief superfusion period used when studying the decay of depolarization-induced suppression of inhibition. Therefore, we propose that endocannabinoid signalling is a key neuromodulatory homeostatic system mediating adaptive responses to neurotoxic insults (Bisogno and Di Marzo, 2008) and defining the dynamics of presynaptic neurotransmitter release under disease conditions.

## 2-Arachidonoyl glycerol signalling in microglia: the good, the bad or the ugly?

Microglia are central to Alzheimer's pathogenesis since their activation state determines whether they are beneficial by phagocytosing cell debris or elicit neuronal injury by releasing pro-inflammatory cytokines. Migrating microglia express CB<sub>2</sub> cannabinoid receptors whose activation suppresses pro-inflammatory cytokine production (Klegeris *et al.*, 2003). Once activated, microglia down-regulate CB<sub>2</sub> cannabinoid receptors, as seen upon WNT-3A challenge, to increase cytokine production. Microglia continuously monitor the functional state of synapses via the dynamic motility of their processes. Disrupting neuron-glia communication (also including astrocytes) (Rodríguez *et al.*, 2009) will therefore culminate in the loss of glial homeostatic control, and facilitate the onset of synaptic deficit. Thus, altered 2-arachidonoyl glycerol signalling in activated microglia can have serious consequences in Alzheimer's disease, particularly since a 2-arachidonoyl glycerol 'overflow' from activated microglia and astrocytes (Scuderi *et al.*, 2011) may be viewed as a volumetric insult indiscriminately affecting synapse populations and assemblies of neurons. Overall, pathogenic modifications to 2-arachidonoyl glycerol metabolism in microglia can exacerbate synaptic impairment in Alzheimer's disease.

## 2-Arachidonoyl glycerol hydrolysis by ABHD6 and monoacylglycerol lipase in Alzheimer's disease

ABHD6 and monoacylglycerol lipase terminate surplus 2-arachidonoyl glycerol to maintain temporally coordinated retrograde signalling (Dinh *et al.*, 2002; Marrs *et al.*, 2010). Alzheimer's pathology will ultimately modify 2-arachidonoyl glycerol signalling if it either impacts the recruitment of ABHD6 and/or monoacylglycerol lipase to signalling positions or compromises their enzymatic activity. We found that AT8<sup>+</sup> neurons cease ABHD6 expression, suggesting impaired postsynaptic 2-arachidonoyl glycerol degradation when the cytoskeletal integrity of neurons becomes compromised. The loss of ABHD6 recruitment may be pathophysiologically significant since it could alter the balance of postsynaptic 2-arachidonoyl glycerol synthesis and degradation such that 2-arachidonoyl glycerol could continuously 'leak' out of subsynaptic dendrites. Thus, the lack of ABHD6-mediated ligand degradation may impair the temporal precision of retrograde signalling.

Monoacylglycerol lipase-dependent 2-arachidonoyl glycerol degradation requires monoacylglycerol lipase's recruitment as a dimer to the internal leaflet of the plasmalemma (Labar *et al.*, 2010). Our findings reveal that monoacylglycerol lipase's association to the plasmalemma is particularly hindered in brains inflicted by Alzheimer's. Instead, monoacylglycerol lipase is sequestered in the cytosol, which we consider incompetent to degrade 2-arachidonoyl glycerol targeting transmembrane receptors and participating in retrograde signalling. We propose that diminished association of monoacylglycerol lipase to the plasmalemma may be due to intracellular acidosis or membrane damage through lipid peroxidation (Querfurth and LaFerla, 2010). Nevertheless, our biochemical data suggest the existence of compensatory mechanisms since the contribution of JZL184 (URB602)-insensitive 2-arachidonoyl glycerol-degrading enzymes is markedly increased in Alzheimer's disease, compatible with our observation of increased ABHD6 expression in microglia and/or astrocytes. We also found that amyloid- $\beta$  is central to regulating both the subcellular localization and activity of monoacylglycerol lipase. The physiological significance of this interaction may be increased intracellular 2-arachidonoyl glycerol degradation preventing receptor-independent antioxidant actions of 2-arachidonoyl glycerol (Bisogno and Di Marzo 2008), thus predisposing neurons to amyloid- $\beta$ -induced oxidative damage.

Previous studies (Ramirez *et al.*, 2005; Chen *et al.*, 2011) demonstrate that cannabinoids may rescue neurons under Alzheimer-like conditions by suppressing pro-inflammatory microglia activity (Ramirez *et al.*, 2005). Our present results uncover novel mechanistic insights in neuronal (synaptic) 2-arachidonoyl glycerol signalling, as well as 2-arachidonoyl glycerol-mediated neuron-glia interactions. We suggest that reduced pre- as well as postsynaptic 2-arachidonoyl glycerol degradation coincident with increased and ectopic 2-arachidonoyl glycerol synthesis can disrupt the temporal and spatial control of retrograde signalling, and—consequently—aggravate synapse impairment in Alzheimer's disease. Therefore, endocannabinoid signalling networks may represent novel targets



to reinstate the precision of synaptic communication under neurodegenerative conditions associated with cognitive deficit.

## Acknowledgements

The authors thank B. Cravatt (The Scripps Research Institute) for monoacylglycerol lipase<sup>-/-</sup> mouse brains, J. Jankowsky and D. Borchelt (John Hopkins University) for colony founders of the APdE9 strain, A. Avelino (University of Porto) for TRPV<sub>1</sub><sup>-/-</sup> mice, W. Härtig (University of Leipzig) for directly conjugated glial fibrillary acidic protein-carbocyanine 3 antibody, B. Penke and L. Fülöp (University of Szeged) for amyloid- $\beta_{1-42}$  peptide, R. Hessling and J. Lindenau (Carl Zeiss) for advice on quantitative immunofluorescence analysis, Y. Zilberter (INSERM U751) and A. Fisahn (Karolinska Institutet) for help with electrophysiology, V. Di Marzo for advice on anti-TRPV<sub>1</sub> antibodies, R.A. Ross (University of Aberdeen), A. Bacci (European Brain Research Institute, Rome) and I. Katona (Institute of Experimental Medicine, Hungarian Academy of Sciences) for constructive criticism and discussions.

## Funding

This work was supported by the Scottish Universities Life Science Alliance (SULSA; THa), European Molecular Biology Organization Young Investigator Programme (THa), Swedish Medical Research Council (GS, THa), Alzheimer's Research Trust UK (THa), Alzheimer's Association (KM, THa), European Commission (HEALTH-F2-2007-201159; HT, THa), National Institutes of Health grants (DA023214 (THa), DA011322 (KM), and DA021696 (KM)), Fundação para a Ciência e a Tecnologia (PTDC/SAU-OSM/105663/2008; AK; SFRH/BD/33467/2008; SGF), the Spanish Ministry of Science and Innovation (SAF2005-02845; MLC) and Madrid Council (S-BIO/0170/2006; MLC). JM and AMM-M received fellowship support from the Alzheimer's Research Trust UK and The Spanish Ministry of Science and Innovation, respectively.

## Supplementary material

Supplementary material is available at *Brain* online.

## References

- Alger BE. Retrograde signaling in the regulation of synaptic transmission: focus on endocannabinoids. *Prog Neurobiol* 2002; 68: 247–86.
- Bell KF, Ducatenzeiler A, Ribeiro-da-Silva A, Duff K, Bennett DA, Cuello AC. The amyloid pathology progresses in a neurotransmitter-specific manner. *Neurobiol Aging* 2006; 27: 1644–57.
- Benito C, Nunez E, Tolon RM, Carrier EJ, Rabano A, Hillard CJ, et al. Cannabinoid CB2 receptors and fatty acid amide hydrolase are selectively overexpressed in neuritic plaque-associated glia in Alzheimer's disease brains. *J Neurosci* 2003; 23: 11136–41.
- Bilkei-Gorzo A, Racz I, Valverde O, Otto M, Michel K, Sastre M, et al. Early age-related cognitive impairment in mice lacking cannabinoid CB1 receptors. *Proc Natl Acad Sci USA* 2005; 102: 15670–5.
- Bisogno T, Di Marzo V. The role of the endocannabinoid system in Alzheimer's disease: facts and hypotheses. *Curr Pharm Des* 2008; 14: 2299–3305.
- Bisogno T, Howell F, Williams G, Minassi A, Cascio MG, Ligresti A, et al. Cloning of the first sn1-DAG lipases points to the spatial and temporal regulation of endocannabinoid signaling in the brain. *J Cell Biol* 2003; 163: 463–8.
- Blankman JL, Simon GM, Cravatt BF. A comprehensive profile of brain enzymes that hydrolyze the endocannabinoid 2-arachidonoylglycerol. *Chem Biol* 2007; 14: 1347–56.
- Blazquez C, Chiarlone A, Sagredo O, Aguado T, Pazos MR, Resel E, et al. Loss of striatal type 1 cannabinoid receptors is a key pathogenic factor in Huntington's disease. *Brain* 2011; 134: 119–36.
- Bradford MM. A rapid and sensitive method for the quantitation of microgram quantities of protein utilizing the principle of protein-dye binding. *Anal Biochem* 1976; 72: 248–54.
- Busche MA, Eichhoff G, Adelsberger H, Abramowski D, Wiederhold KH, Haass C, et al. Clusters of hyperactive neurons near amyloid plaques in a mouse model of Alzheimer's disease. *Science* 2008; 321: 1686–9.
- Chen X, Zhang J, Chen C. Endocannabinoid 2-arachidonoylglycerol protects neurons against beta-amyloid insults. *Neuroscience* 2011; 178: 159–68.
- Cravatt BF, Giang DK, Mayfield SP, Boger DL, Lerner RA, Gilula NB. Molecular characterization of an enzyme that degrades neuromodulatory fatty-acid amides. *Nature* 1996; 384: 83–7.
- Dinh TP, Carpenter D, Leslie FM, Freund TF, Katona I, Sensi SL, et al. Brain monoglyceride lipase participating in endocannabinoid inactivation. *Proc Natl Acad Sci U S A* 2002; 99: 10819–24.
- Gao Y, Vasilyev DV, Goncalves MB, Howell FV, Hobbs C, Reisenberg M, et al. Loss of retrograde endocannabinoid signaling and reduced adult neurogenesis in diacylglycerol lipase knock-out mice. *J Neurosci* 2010; 30: 2017–24.
- Garbelli R, Inverardi F, Medici V, Amadeo A, Verderio C, Matteoli M, et al. Heterogeneous expression of SNAP-25 in rat and human brain. *J Comp Neurol* 2008; 506: 373–86.
- Goedert M, Spillantini MG, Jakes R, Rutherford D, Crowther RA. Multiple isoforms of human microtubule-associated protein tau: sequences and localization in neurofibrillary tangles of Alzheimer's disease. *Neuron* 1989; 3: 519–26.
- Gu Z, Liu W, Yan Z.  $\beta$ -Amyloid impairs AMPA receptor trafficking and function by reducing Ca<sup>2+</sup>/calmodulin-dependent protein kinase II synaptic distribution. *J Biol Chem* 2009; 284: 10639–49.
- Halleskog C, Mulder J, Dahlstrom J, Mackie K, Hortobagyi T, Tanila H, et al. WNT signaling in activated microglia is proinflammatory. *Glia* 2011; 59: 119–31.
- Harkany T, Dobszay MB, Cayetanot F, Hartig W, Siegemund T, Aujard F, et al. Redistribution of CB1 cannabinoid receptors during evolution of cholinergic basal forebrain territories and their cortical projection areas: a comparison between the gray mouse lemur (*Microcebus murinus*, primates) and rat. *Neuroscience* 2005; 135: 595–609.
- Harkany T, Hartig W, Berghuis P, Dobszay MB, Zilberter Y, Edwards RH, et al. Complementary distribution of type 1 cannabinoid receptors and vesicular glutamate transporter 3 in basal forebrain suggests input-specific retrograde signalling by cholinergic neurons. *Eur J Neurosci* 2003; 18: 1979–92.
- Hashimoto-dani Y, Ohno-Shosaku T, Kano M. Presynaptic monoacylglycerol lipase activity determines basal endocannabinoid tone and terminates retrograde endocannabinoid signaling in the hippocampus. *J Neurosci* 2007; 27: 1211–9.
- Hauser WA, Morris ML, Heston LL, Anderson VE. Seizures and myoclonus in patients with Alzheimer's disease. *Neurology* 1986; 36: 1226–30.
- Hsieh H, Boehm J, Sato C, Iwatsubo T, Tomita T, Sisodia S, et al. AMPAR removal underlies Abeta-induced synaptic depression and dendritic spine loss. *Neuron* 2006; 52: 831–43.
- Jankowsky JL, Fadale DJ, Anderson J, Xu GM, Gonzales V, Jenkins NA, et al. Mutant presenilins specifically elevate the levels of the 42 residue

- beta-amyloid peptide *in vivo*: evidence for augmentation of a 42-specific gamma secretase. *Hum Mol Genet* 2004; 13: 159–70.
- Jung KM, Astarita G, Zhu C, Wallace M, Mackie K, Piomelli D. A key role for diacylglycerol lipase- $\alpha$  in metabotropic glutamate receptor-dependent endocannabinoid mobilization. *Mol Pharmacol* 2007; 72: 612–21.
- Kamenetz F, Tomita T, Hsieh H, Seabrook G, Borchelt D, Iwatsubo T, et al. APP processing and synaptic function. *Neuron* 2003; 37: 925–37.
- Kano M, Ohno-Shosaku T, Hashimoto-dani Y, Uchigashima M, Watanabe M. Endocannabinoid-mediated control of synaptic transmission. *Physiol Rev* 2009; 89: 309–80.
- Katona I, Urban GM, Wallace M, Ledent C, Jung KM, Piomelli D, et al. Molecular composition of the endocannabinoid system at glutamatergic synapses. *J Neurosci* 2006; 26: 5628–37.
- Kawamura Y, Fukaya M, Maejima T, Yoshida T, Miura E, Watanabe M, et al. The CB1 cannabinoid receptor is the major cannabinoid receptor at excitatory presynaptic sites in the hippocampus and cerebellum. *J Neurosci* 2006; 26: 2991–3001.
- Keimpema E, Barabas K, Morozov YM, Tortoriello G, Torii M, Cameron G, et al. Differential subcellular recruitment of monoacylglycerol lipase generates spatial specificity of 2-arachidonoyl glycerol signaling during axonal pathfinding. *J Neurosci* 2010; 30: 13992–4007.
- Khaspekov LG, Brenz Verca MS, Frumkina LE, Hermann H, Marsicano G, Lutz B. Involvement of brain-derived neurotrophic factor in cannabinoid receptor-dependent protection against excitotoxicity. *Eur J Neurosci* 2004; 19: 1691–8.
- King AR, Duranti A, Tontini A, Rivara S, Rosengarth A, Clapper JR, et al. URBraak stage VI02 inhibits monoacylglycerol lipase and selectively blocks 2-arachidonoylglycerol degradation in intact brain slices. *Chem Biol* 2007; 14: 1357–65.
- Klegeris A, Bissonnette CJ, McGee PL. Reduction of human monocytic cell neurotoxicity and cytokine secretion by ligands of the cannabinoid-type CB2 receptor. *Br J Pharmacol* 2003; 139: 775–86.
- Kofalvi A, Pereira MF, Rebola N, Rodrigues RJ, Oliveira CR, Cunha RA. Anandamide and NADA bi-directionally modulate presynaptic  $\text{Ca}^{2+}$  levels and transmitter release in the hippocampus. *Br J Pharmacol* 2007; 151: 551–63.
- Kuchibhotla KV, Goldman ST, Lattarulo CR, Wu HY, Hyman BT, Bacskai BJ. Abeta plaques lead to aberrant regulation of calcium homeostasis *in vivo* resulting in structural and functional disruption of neuronal networks. *Neuron* 2008; 59: 214–25.
- Labar G, Bauvois C, Borel F, Ferrer JL, Wouters J, Lambert DM. Crystal structure of the human monoacylglycerol lipase, a key actor in endocannabinoid signaling. *ChemBiochem* 2010; 11: 218–27.
- Lacor PN, Buniel MC, Chang L, Fernandez SJ, Gong Y, Viola KL, et al. Synaptic targeting by Alzheimer's-related amyloid beta oligomers. *J Neurosci* 2004; 24: 10191–200.
- Lastres-Becker I, Molina-Holgado F, Ramos JA, Mechoulam R, Fernandez-Ruiz J. Cannabinoids provide neuroprotection against 6-hydroxydopamine toxicity *in vivo* and *in vitro*: relevance to Parkinson's disease. *Neurobiol Dis* 2005; 19: 96–107.
- Lee JH, Agacinski G, Williams JH, Wilcock GK, Esiri MM, Francis PT, et al. Intact cannabinoid CB1 receptors in the Alzheimer's disease cortex. *Neurochem Int* 2010; 57: 985–9.
- Long JZ, Li W, Booker L, Burston JJ, Kinsey SG, Schlosburg JE, et al. Selective blockade of 2-arachidonoylglycerol hydrolysis produces cannabinoid behavioral effects. *Nat Chem Biol* 2009; 5: 37–44.
- Ludanyi A, Eross L, Czirkak S, Vajda J, Halasz P, Watanabe M, et al. Down-regulation of the CB1 cannabinoid receptor and related molecular elements of the endocannabinoid system in epileptic human hippocampus. *J Neurosci* 2008; 28: 2976–90.
- Ludanyi A, Hu SS, Yamazaki M, Tanimura A, Piomelli D, Watanabe M, et al. Complementary synaptic distribution of enzymes responsible for synthesis and inactivation of the endocannabinoid 2-arachidonoylglycerol in the human hippocampus. *Neuroscience* 2011; 174: 50–63.
- Marrs WR, Blankman JL, Horne EA, Thomazeau A, Lin YH, Coy J, et al. The serine hydrolase ABHD6 controls the accumulation and efficacy of 2-arachidonoyl glycerol at cannabinoid receptors. *Nat Neurosci* 2010; 13: 951–7.
- Mattson MP, Chan SL. Neuronal and glial calcium signaling in Alzheimer's disease. *Cell Calcium* 2003; 34: 385–97.
- Mazzola C, Micale V, Drago F. Amnesia induced by beta-amyloid fragments is counteracted by cannabinoid CB1 receptor blockade. *Eur J Pharmacol* 2003; 477: 219–25.
- Micale V, Cristino L, Tamburella A, Petrosino S, Leggio GM, Di Marzo V, et al. Enhanced cognitive performance of dopamine D3 receptor 'knock-out' mice in the step-through passive-avoidance test: assessing the role of the endocannabinoid/endovanilloid systems. *Pharmacol Res* 2010; 61: 531–6.
- Minkeviciene R, Rheims S, Dobszay MB, Zilberter M, Hartikainen J, Fulop L, et al. Amyloid beta-induced neuronal hyperexcitability triggers progressive epilepsy. *J Neurosci* 2009; 29: 3453–62.
- Mor M, Rivara S, Lodola A, Plazzi PV, Tarzia G, Duranti A, et al. Cyclohexylcarbamic acid 3'- or 4'-substituted biphenyl-3-yl esters as fatty acid amide hydrolase inhibitors: synthesis, quantitative structure-activity relationships, and molecular modeling studies. *J Med Chem* 2004; 47: 4998–5008.
- Nomura DK, Long JZ, Niessen S, Hoover HS, Ng SW, Cravatt BF. Monoacylglycerol lipase regulates a fatty acid network that promotes cancer pathogenesis. *Cell* 2010; 140: 49–61.
- Nunez E, Benito C, Tolon RM, Hillard CJ, Griffin WS, Romero J. Glial expression of cannabinoid CB(2) receptors and fatty acid amide hydrolase are beta amyloid-linked events in Down's syndrome. *Neuroscience* 2008; 151: 104–10.
- Oddo S, Caccamo A, Shepherd JD, Murphy MP, Golde TE, Kaye R, et al. Triple-transgenic model of Alzheimer's disease with plaques and tangles: intracellular Abeta and synaptic dysfunction. *Neuron* 2003; 39: 409–21.
- Palazuelos J, Aguado T, Pazos MR, Julien B, Carrasco C, Resel E, et al. Microglial CB2 cannabinoid receptors are neuroprotective in Huntington's disease excitotoxicity. *Brain* 2009; 132: 3152–64.
- Peng I, Binder LI, Black MM. Biochemical and immunological analyses of cytoskeletal domains of neurons. *J Cell Biol* 1986; 102: 252–62.
- Querfurth HW, LaFerla FM. Alzheimer's disease. *N Engl J Med* 2010; 362: 329–44.
- Ramirez BG, Blazquez C, del Pulgar TG, Guzman N, de Ceballos MAL. Prevention of Alzheimer's disease pathology by cannabinoids: neuroprotection mediated by blockade of microglial activation. *J Neurosci* 2005; 25: 1904–13.
- Rodriguez JJ, Olabarria M, Chvatal A, Verkhratsky A. Astroglia in dementia and Alzheimer's disease. *Cell Death Differ* 2009; 16: 378–85.
- Roloff AM, Anderson GR, Martemyanov KA, Thayer SA. Homer 1a gates the induction mechanism for endocannabinoid-mediated synaptic plasticity. *J Neurosci* 2010; 30: 3072–81.
- Roselli F, Hutzler P, Wegerich Y, Livrea P, Almeida OF. Disassembly of shank and homer synaptic clusters is driven by soluble beta-amyloid(1–40) through divergent NMDAR-dependent signalling pathways. *PLoS One* 2009; 4: e6011.
- Sampedro MN, Bussineau CM, Cotman CW. Turnover of brain postsynaptic densities after selective deafferentation: detection by means of an antibody to antigen PSD-95. *Brain Res* 1982; 251: 211–20.
- Schlosburg JE, Blankman JL, Long JZ, Nomura DK, Pan B, Kinsey SG, et al. Chronic monoacylglycerol lipase blockade causes functional antagonism of the endocannabinoid system. *Nat Neurosci* 2010; 13: 1113–9.
- Schubert W, Prior R, Weidemann A, Dirksen H, Multhaup G, Masters CL, et al. Localization of Alzheimer beta A4 amyloid precursor protein at central and peripheral synaptic sites. *Brain Res* 1991; 563: 184–94.
- Scuderi C, Esposito G, Blasio A, Valenza M, Arietti P, Steardo L Jr, et al. Palmitoylethanolamide counteracts reactive astrogliosis induced by beta-amyloid peptide. *J Cell Mol Med* 2011; doi: 10.1111/j.1582-4934.2011.01267.x.

- Shemer I, Holmgren C, Min R, Fulop L, Zilberter M, Sousa KM, et al. Non-fibrillar beta-amyloid abates spike-timing-dependent synaptic potentiation at excitatory synapses in layer 2/3 of the neocortex by targeting postsynaptic AMPA receptors. *Eur J Neurosci* 2006; 23: 2035–47.
- Simon GM, Cravatt BF. Anandamide biosynthesis catalyzed by the phosphodiesterase GDE1 and detection of glycerophospho-N-acyl ethanolamine precursors in mouse brain. *J Biol Chem* 2008; 283: 9341–9.
- Small SA, Duff K. Linking A $\beta$  and tau in late-onset Alzheimer's disease: a dual pathway hypothesis. *Neuron* 2008; 60: 534–42.
- Snyder EM, Nong Y, Almeida CG, Paul S, Moran T, Choi EY, et al. Regulation of NMDA receptor trafficking by amyloid- $\beta$ . *Nat Neurosci* 2005; 8: 1051–8.
- Tanimura A, Yamazaki M, Hashimoto-dani Y, Uchigashima M, Kawata S, Abe M, et al. The endocannabinoid 2-arachidonoylglycerol produced by diacylglycerol lipase  $\alpha$  mediates retrograde suppression of synaptic transmission. *Neuron* 2010; 65: 320–7.
- Uchigashima M, Narushima M, Fukaya M, Katona I, Kano M, Watanabe M. Subcellular arrangement of molecules for 2-arachidonoyl-glycerol-mediated retrograde signaling and its physiological contribution to synaptic modulation in the striatum. *J Neurosci* 2007; 27: 3663–76.
- Ueda N, Okamoto Y, Morishita J. N-acylphosphatidylethanolamine-hydrolyzing phospholipase D: a novel enzyme of the beta-lactamase fold family releasing anandamide and other N-acylethanolamines. *Life Sci* 2005; 77: 1750–8.
- van der Stelt M, Mazzola C, Esposito G, Matias I, Petrosino S, De Filippis D, et al. Endocannabinoids and beta-amyloid-induced neurotoxicity in vivo: effect of pharmacological elevation of endocannabinoid levels. *Cell Mol Life Sci* 2006; 63: 1410–24.
- Walsh DM, Klyubin I, Fadeeva JV, Cullen WK, Anwyl R, Wolfe MS, et al. Naturally secreted oligomers of amyloid  $\beta$  protein potently inhibit hippocampal long-term potentiation in vivo. *Nature* 2002; 416: 535–9.
- Walsh DM, Selkoe DJ. Deciphering the molecular basis of memory failure in Alzheimer's disease. *Neuron* 2004; 44: 181–93.
- Walter L, Franklin A, Witting A, Wade C, Xie Y, Kunos G, et al. Nonpsychotropic cannabinoid receptors regulate microglial cell migration. *J Neurosci* 2003; 23: 1398–405.
- Westlake TM, Howlett AC, Bonner TI, Matsuda LA, Herkenham M. Cannabinoid receptor binding and messenger RNA expression in human brain: an in vitro receptor autoradiography and in situ hybridization histochemistry study of normal aged and Alzheimer's brains. *Neuroscience* 1994; 63: 637–52.
- Wise LE, Thorpe AJ, Lichtman AH. Hippocampal CB(1) receptors mediate the memory impairing effects of Delta(9)-tetrahydrocannabinol. *Neuropsychopharmacology* 2009; 34: 2072–80.
- Xu H, Chen M, Manivannan A, Lois N, Forrester JV. Age-dependent accumulation of lipofuscin in perivascular and subretinal microglia in experimental mice. *Aging Cell* 2008; 7: 58–68.
- Yoles E, Belkin M, Schwartz M. HU-211, a nonpsychotropic cannabinoid, produces short- and long-term neuroprotection after optic nerve axotomy. *J Neurotrauma* 1996; 13: 49–57.
- Yoshida T, Fukaya M, Uchigashima M, Miura E, Kamiya H, Kano M, et al. Localization of diacylglycerol lipase- $\alpha$  around postsynaptic spine suggests close proximity between production site of an endocannabinoid, 2-arachidonoyl-glycerol, and presynaptic cannabinoid CB1 receptor. *J Neurosci* 2006; 26: 4740–51.